

Chapter 5

Connections between neurons

A single neuron can be a powerful computational device in its own right. Yet it is the huge number of interconnected neurons that gives the brains of higher organisms such as humans their immense capabilities. Estimates for the human brain suggest we possess over 80 billion neurons with more than 1000-fold that number of connections. The pattern of those connections is essential for our ability to respond appropriately to the outside world, to recall memories, and to plan for the future. In Chapter 8, we will consider how those connections change through learning and development via the process of synaptic plasticity. In the current chapter, we will consider the operation of individual connections, how one neuron can affect another through its connections, and how two or three interconnected neurons give rise to useful behavior in a small circuit.

5.1. The synapse

Neurons connect with each other through *synapses* (from two Greek words meaning “fastened together”). Two types of synapse, chemical and electrical, are physically distinct in their operation. Chemical synapses can also be subdivided into excitatory and inhibitory synapses, based on their functional effect.

Box 5.1. Synapse: A connection between two cells.

5.1.1. Electrical synapses

Electrical synapses contain a direct, physical connection between two neurons called a gap junction. The junction contains small pores, through which ions can flow. In the simplest case the gap junction can be modeled as a resistor, such that a constant conductance is added between the two cells in the same manner as between adjoining compartments of a multi-compartment model. In other cases, the gap junction can be rectifying, meaning it only allows current to pass in one direction. In this case, the conductance is dependent on the voltage-difference across the junction and is set to zero if one neuron has a higher membrane potential than the other.

Box 5.2. Gap junction: A connection between two cells, across which ions can directly flow.

5.1.2. Chemical synapses

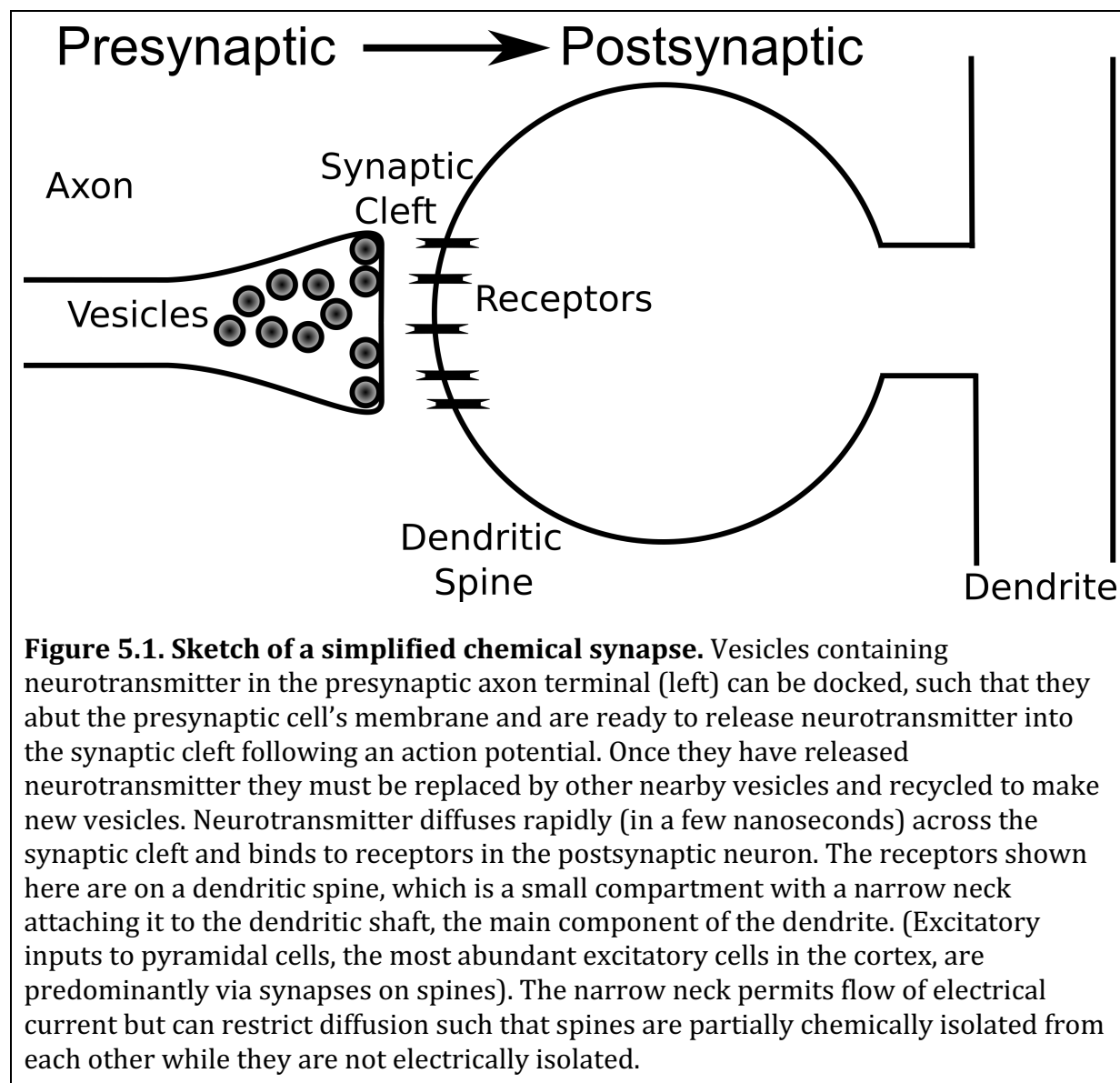
Chemical synapses are the most common type in mammalian brains. Two neurons connected by a chemical synapse are separated by a small gap, the *synaptic cleft* (Figure 5.1). Interaction between the two neurons is via the release of chemicals called *neurotransmitters*. The dominant method of interaction is unidirectional, from the axon terminal of a presynaptic neuron to the dendritic spine, dendritic shaft or soma of a postsynaptic neuron.

Box 5.3. Neurotransmitter: The general term for any chemical that diffuses across the space between two neurons, allowing communication between them.

Box 5.4. Presynaptic neuron: Referring to a particular synapse, the presynaptic neuron is the neuron that releases neurotransmitter across the synapse when it produces an action potential.

Box 5.5. Postsynaptic neuron: Referring to a particular synapse, the postsynaptic neuron is the neuron that responds to neurotransmitter following an action potential in the presynaptic neuron.

Box 5.6. Vesicles: Tiny compartments surrounded by membrane, which contain particular chemicals, such as neurotransmitter, to be transported or released outside the cell.



When the presynaptic neuron produces an action potential, the voltage spike is transmitted along the axon, which is typically very branched, generating a spike in the membrane potential at all of its axon terminals. The voltage spike causes high-threshold

(N-type “neural” and P/Q-type “Purkinje”) calcium channels in the vicinity of the axon terminal to open. The ensuing calcium influx initiates activation of proteins, which eventually cause *vesicles* (small, membrane-enclosed spherical containers) containing neurotransmitter to release their payload into the synaptic cleft¹. The neurotransmitter diffuses across the small gap between cells and binds to receptors of the postsynaptic cell. When the receptors are bound by neurotransmitter they cause channels to open, either directly through a conformational change if they are ionotropic, or indirectly through a signaling pathway if they are metabotropic. The open channels cause electric current to flow, either into or out of the cell depending on the ion that flows, just as is the case with other ion channels in the cell membrane.

Box 5.7. Receptor: A protein that can be bound by a signaling molecule (such as a neurotransmitter) and, when bound, either activates or changes its conformation in order to produce further change.

The series of steps described in the above paragraph (which omits several intermediate steps that provide fodder for many research careers) can seem like an overly tortuous pathway for one neuron to affect another. Amazingly, all of these biochemical processes and the intervening step of chemical diffusion can be completed within a millisecond, in part because they take place in a tiny volume of space. Indeed, when we simulate the interaction between two neurons it is common to treat the time from the action potential of one neuron to the conductance change in another as negligible. If any delays are added in simulations, typically these are due to propagation of the action potential from the soma to the end of the axon, or (either passive or active) propagation of the postsynaptic voltage change from a distal dendrite to the soma. Such delays may be important when considering spike-time dependent plasticity (Section 8.3) in which the change in strength of a synapse can depend sensitively on the relative timings of a presynaptic and a postsynaptic spike.

The series of biochemical processes involved in synaptic transmission gives rise to some important computational consequences. The first is a short-term history dependence of the synaptic efficacy, which we will consider in Section 5.3. The second is the introduction of randomness or noise, because an action potential does not guarantee the release of a vesicle of neurotransmitter, which depends on several proteins binding to the vesicle or activating vesicle-release machinery in concert. These stochastic biochemical reactions—whose ultimate source of randomness is the bouncing around of molecules due to thermal energy—are likely the major source of random variability in membrane potentials *in vivo* and hence, ultimately, a source of variability in animal behavior.

If there are many vesicles near the synaptic cleft, the variability in neurotransmission is reduced. For example, in the end plate junction—the connection between motor neurons and muscle fiber—many hundreds of vesicles can be released. This is important, as while we may not want perfect predictability in some of our thought processes, when we need to jump out of the way of a car, our leg muscles must be guaranteed to contract!

Synapses in the retina and in many invertebrates with thousands of vesicles allow for continuous and *graded release* of neurotransmitter, so that small changes in the

membrane potential of a presynaptic cell can impact the current flow into a postsynaptic cell in the absence of any action potential.

Box 5.8. Motor neuron: A neuron that helps control an animal's movement.

Box 5.9. Graded release: Neurotransmitter release at a rate that can increase or decrease according to the presynaptic membrane potential.

The most important feature of a chemical synapse is whether synaptic transmission causes an increase or a decrease of the postsynaptic membrane potential. Synapses that cause a depolarization are *excitatory*, while synapses that cause a hyperpolarization or reduce any depolarization are *inhibitory*. Whether a synapse is excitatory or inhibitory depends on the neurotransmitter being released and the receptors in the postsynaptic cell. The effects of a neurotransmitter can be qualitatively different across species and even across the course of development between the same two cells when reversal potentials (*i.e.*, equilibrium potentials) change due to changes in ionic concentrations (see Eq. 2.1, the Nernst Equation).

Box 5.10. Excitatory synapse: A synapse causing depolarization of the postsynaptic cell.

Box 5.11. Inhibitory synapse: A synapse causing hyperpolarization of the postsynaptic cell.

Box 5.12. Dale's Principle: All synapses of a presynaptic cell release the same types of neurotransmitter, sometimes extended to denote the situation in particular circuits where neurons are either only excitatory or only inhibitory in their effect on other cells.

Dale's Principle states that the neurotransmitters released by a neuron at one synapse are the same as the neurotransmitters released by that neuron at another synapse. That is, while most neurons have synapse-specific receptors, receiving different types of input from different types of presynaptic cells, they typically have the same type of output at all axon terminals. In this form, Dale's Principle has very few exceptions, but it is commonly rephrased to state, incorrectly in general, that a presynaptic cell provides only excitatory or only inhibitory input to other cells. In some circuits the latter statement is true, in which case it is convenient to classify neurons as excitatory or inhibitory according to the neurotransmitter that they release most abundantly.

The reason such classification is an oversimplification is two-fold. First, many neurotransmitters have mixed effects—*i.e.*, whether they excite a cell or inhibit it can depend on the postsynaptic receptor, the excitatory D1 and inhibitory D2 receptors for dopamine being the best-known example^{2,3}. Second, neurons can release different types of, often modulatory, neurotransmitters together in a process called cotransmission, so the postsynaptic effects depend on the relative abundance of receptors to the different neurotransmitters.

It is reasonable to label a cell as either excitatory or inhibitory, when it packages just one type of neurotransmitter at its axon terminals and if, when that neurotransmitter can

bind to more than one type of postsynaptic receptor, the different receptors cause qualitatively the same postsynaptic effect.

Box 5.13. Glutamate: The dominant excitatory neurotransmitter in mammals.

Box 5.14. AMPA receptor: A receptor, which when bound by glutamate produces a rapid excitatory response in the postsynaptic cell.

Box 5.15. NMDA receptor: A receptor, which when bound by glutamate, and when the postsynaptic membrane potential is high, produces a slower excitatory response in the postsynaptic cell.

Box 5.16. γ -Aminobutyric acid (GABA): The dominant inhibitory neurotransmitter in mammals.

For example, the most common neurotransmitter released by excitatory cells in mammalian cortex is glutamate. Glutamate binds to two common receptors that are expressed together in postsynaptic cells, N-methyl-D-aspartate (NMDA) receptors and α -amino-3-hydroxy-5-methyl-4-isoxazolepropionic acid (AMPA) receptors. The two receptors each cause excitatory channels to open, allowing flow of a mixture of positive ions (cations) with a net flux into the cell, but otherwise they have distinct properties. AMPA receptors respond rapidly to glutamate binding, opening almost instantaneously and closing over a time-scale of a couple of milliseconds. NMDA receptors have slower dynamics and are able to remain open for many tens of milliseconds. They also admit calcium ions, which can be important for biochemical signaling and they contain a magnesium block that requires postsynaptic depolarization to be released. Thus, their conductance depends not only on when the presynaptic cell spiked but also on the membrane potential of the postsynaptic cell. Still, while glutamate mediates excitatory synaptic transmission in mammalian brains, it is worth noting that it has an inhibitory effect in many insect brains where it causes chloride channels to open.

The most common inhibitory neurotransmitter in mammalian brains is γ -Aminobutyric acid (GABA). The receptors for GABA cause chloride channels to open. Chloride ions are in higher concentration outside the cell, so they flow into the cell unless the cell is hyperpolarized. While the reversal potential of chloride channels is always negative, early in development it can be far enough above the resting membrane potential for the chloride current to be outward and have an excitatory effect on neurons. Later in development the reversal potential drops toward the resting potential or below—certainly far from threshold—such that channel opening produces an inhibitory effect on the postsynaptic cell.

In this book, we will follow the simplified rule of cells being either excitatory or inhibitory, because such a rule describes the dominant interactions in the circuits that we focus on. However, the reader should be aware of the existence of many exceptions, more of which are likely to be discovered each year.

5.2. Modeling synaptic transmission through chemical synapses

The effect of synaptic transmission can be simulated via the synaptic conductance in the postsynaptic cell. Just as we saw that sodium conductance and potassium conductance were treated separately in single-cell models, so too must each type of synaptic conductance be treated with a separate term in the differential equation. Different receptors of neurotransmitter cause channels to open and close with different dynamics and these channels may admit different ions with different reversal potentials. It is important to note that it is the reversal potential of the ion channels that determines whether a synapse is excitatory or inhibitory—even if those channels allow flow of negative ions, their conductance is always positive when they open.

The general form of the equation for current admitted to a cell due to a particular synaptic conductance is (*cf.* Eq. 2.2):

$$I_{syn}(t) = G_{syn}(t)[V_{syn} - V(t)] \quad \text{Eq. 5.1}$$

where V_{syn} is the reversal potential, $G_{syn}(t)$ is the synaptic conductance which depends primarily on the presynaptic neuron, and $V(t)$ is the membrane potential of the postsynaptic neuron. As always, the parentheses (t) in the term $G_{syn}(t)$, as in the terms $I_{syn}(t)$ and $V(t)$, are optional and are used to indicate a quantity that varies with time.

5.2.1. Spike-induced transmission

The simplest time-dependence for $G_{syn}(t)$ is a step increase at the time of a presynaptic spike, followed by an exponential decay back to zero. This can be modeled by:

$$\frac{dG_{syn}(t)}{dt} = \frac{-G_{syn}(t)}{\tau_{syn}} \quad \text{Eq. 5.2}$$

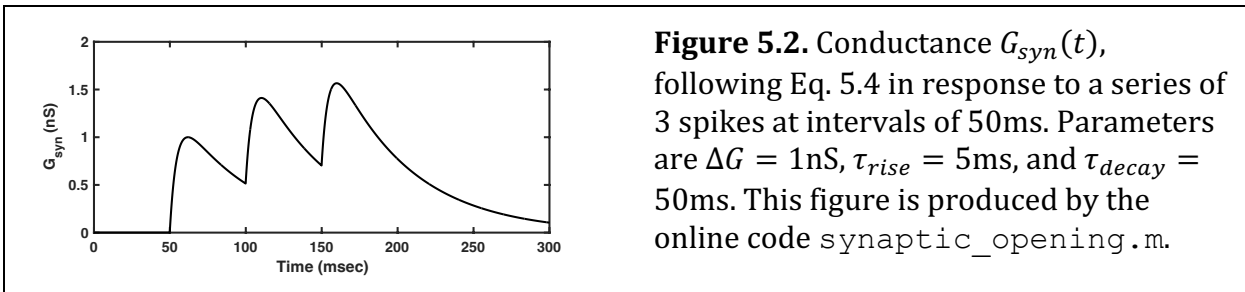
and

$$G_{syn}(t) \mapsto G(t) + \Delta G \text{ if } t \in \{t_{spike}\}, \quad \text{Eq. 5.3}$$

where $\{t_{spike}\}$ is the set of presynaptic spike times so the term $t \in \{t_{spike}\}$ (literally “ t is a member of that set”) simply means add ΔG whenever t is the time of a presynaptic spike. Eq. 5.2 produces exponential decay to zero with a time constant, τ_{syn} , that is specific to the type of synapse. We will be simulating the above model of synaptic transmission in Tutorial 5.1.

The above equations for synaptic transmission are particularly conducive to large-scale simulations because once the conductance is incremented following a presynaptic spike, no further memory of that spike time is needed—the ensuing change in postsynaptic conductance only depends on its value at that time, not the earlier time of the spike. Moreover, the equation for rate of change of conductance (Eq. 5.2) is linear, so the effects of all synapses of a given type within a compartment can be summed together and a single equation (exactly like Eq. 5.2) solved for their net effect—*i. e.*, we do not need to keep track of the conductance of each individual synapse.

One simplification in the above model is the immediate step increase in conductance. This could be mitigated by incorporation of a delay from presynaptic spike to the time of the step increase, without reducing the computational ease of combining multiple synapse-specific conductance terms into one total. However, a more realistic method, particularly for NMDA receptor-mediated channels with their slow time constant, is addition of a rise time to the model of the channel conductance.



An example of a method with such a rise time, shown in Figure 5.2, is a simulation of the dynamics of the conductance following a presynaptic spike as:

$$\Delta G_{syn}(t) = \frac{\Delta G}{K} e^{-(t-t_{spike})/\tau_{decay}} [1 - e^{-(t-t_{spike})/\tau_{rise}}], \quad \text{Eq. 5.4}$$

where τ_{rise} is the rise time and τ_{decay} is the decay time such that $\tau_{decay} > \tau_{rise}$. The factor K is included to ensure the peak height of the conductance change is ΔG . A bit of math (the interested reader can show this for herself) yields $K = \left(\frac{\tau_{decay}}{\tau_{rise} + \tau_{decay}}\right) \left(\frac{\tau_{rise}}{\tau_{rise} + \tau_{decay}}\right)^{\tau_{rise}/\tau_{decay}}$.

In simulations with this method, each spike produces a change in $G_{syn}(t)$ that must be calculated either once for all later times at the time of the spike, or on each succeeding time point using the time of that earlier spike. Once the above formula has been used to calculate the contribution, $\Delta G_{syn}(t)$, from each spike, those contributions are summed together to produce $G_{syn}(t)$. Clearly the realistic method is more involved than the simple method but it will be useful to see how to incorporate it into codes in Tutorial 5.1. Except in situations where the precise timing of spikes is very important (*e.g.*, in sound-source localization or in cases where network synchronization is possible) the simpler method should be fine—but one should always check if a simulated circuit's behavior depends on such simplifications.

5.2.2. Graded release

Neurotransmitter release is always voltage-dependent, in the sense that it depends on calcium influx through voltage-gated calcium channels. However, in most neurons that produce discrete, fast action potentials, the membrane potential at the axon terminal only ever rises above the threshold for calcium influx at the discrete times of spikes. Until now we have just considered the modeling of such all-or-none events.

However, many neurons, for example in invertebrates and in the retina, can release neurotransmitter in a graded, voltage-dependent manner in the absence of a spike. A simple model of channel opening due to graded release of neurotransmitter consists of a synaptic conductance variable with a voltage-dependent steady state and voltage-dependent time constant for its approach to the steady state^{4,5}:

$$\frac{dG_{syn}(t)}{dt} = \frac{G_{\infty}(V_{pre}) - G_{syn}(t)}{\tau_{syn}(V_{pre})}. \quad \text{Eq. 5.5}$$

In some ways, this provides current to a cell in a similar manner to a persistent conductance (such as the potassium conductance of Eq. 4.9 if the synapse is inhibitory, or the calcium conductance of Eq. 4.20 if the synapse is excitatory). However, since we are modeling a synaptic conductance here, its steady state during release is given as a positive

monotonic function of the presynaptic (not postsynaptic) membrane potential. For example,

$$G_{\infty}(V_{pre}) = \frac{G^{(\max)}}{1 + \exp\left[\frac{-(V_{pre} - V_{th})}{V_{range}}\right]} \quad \text{Eq. 5.6}$$

produces a synaptic conductance that can be maintained over a range from zero to its maximum, $G^{(\max)}$, while the presynaptic voltage, V_{pre} , varies over a range of order V_{range} around V_{th} (Figure 5.3A).

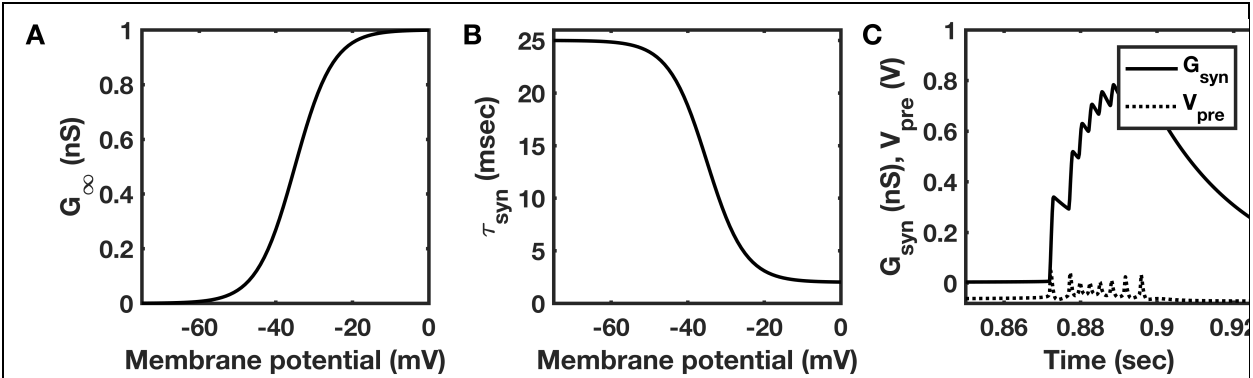


Figure 5.3. Model of synaptic transmission by graded release. **A.** Steady-state conductance is a continuous function of presynaptic membrane potential. **B.** Time constant is slow for unbinding of neurotransmitter at low presynaptic membrane potential and fast for binding at high presynaptic membrane potential. **C.** Response of the model synaptic conductance (solid) to a single burst of presynaptic spikes (dotted, produced by the Pinsky-Rinzel model, Figure 3.15). Parameters for this figure are $G^{(\max)} = 1\text{nS}$, $V_{th} = -35\text{mV}$, $V_{range} = 5\text{mV}$, $\tau_{decay} = 25\text{ms}$, and $\tau_{rise} = 2\text{ms}$. This figure is produced by the online code `graded_release.m` and the file `PR_VS.mat`.

The time constant is modeled so that the conductance increases quickly with a rise in V_{pre} , but falls more slowly when V_{pre} decreases (Figure 5.3B-C):

$$\begin{aligned} \tau_{syn}(V_{pre}) &= \tau_{rise} + (\tau_{decay} - \tau_{rise}) \left[1 - \frac{G(V_{pre})}{G^{(\max)}} \right] \\ &= \tau_{rise} + \frac{(\tau_{decay} - \tau_{rise})}{1 + \exp\left[\frac{(V_{pre} - V_{th})}{V_{range}}\right]}. \end{aligned} \quad \text{Eq. 5.7}$$

Eq. 5.7 models the rapid binding of neurotransmitter once released to produce rapid opening of channels, which can remain open for some time without further neurotransmitter release.

5.3. Dynamical Synapses

We use the term dynamical synapse here to refer to the rapid change in the effective strength of a synaptic connection that arises following each spike and recovers on short

timescales—typically over hundreds of milliseconds, but occasionally over tens of seconds. Such variation is commonly referred to as short-term plasticity⁶⁻⁹, but in this book, we reserve the term “plasticity” for changes that persist (Chapter 8).

Box 5.17. Dynamical synapse: A synapse whose effective strength varies on a short timescale due to the history of incoming action potentials and vesicle release.

Box 5.18. Short-term synaptic depression: A temporary reduction in synaptic strength.

Box 5.19. Short-term synaptic facilitation: A temporary increase in synaptic strength.

5.3.1. Short-term synaptic depression

When a certain number of vesicles release their neurotransmitter from the axon terminal, the number of release-ready vesicles must immediately decrease by that number. Such a reduction in the number of release-ready vesicles causes a reduction in the synaptic transmission produced by an action potential arriving immediately after vesicle release. Therefore, if one action potential were to immediately follow another, all other things being equal, the second action potential would produce a weaker increase in postsynaptic conductance. Such immediate reduction in synaptic efficacy following an action potential is called synaptic depression.

The reduced efficacy typically recovers on a timescale of 100-200 milliseconds, the timescale over which other full vesicles dock in the membrane to become release-ready. Synaptic depression is strong in those synapses with a high baseline probability of release such that a first action potential may cause a substantial reduction in the number of docked vesicles.

Box 5.20. Saturation: The maximum level of a process at which no further increase is possible.

Short-term depression can cause synaptic transmission to depend more strongly on changes in the firing rate of a presynaptic cell than on its stable level of activity. In particular, if a presynaptic neuron is very active, synaptic depression leads to a saturation of synaptic transmission—the rate of neurotransmitter release becomes limited by the rate at which vesicles full of neurotransmitter can dock at the axon terminal rather than the rate of incoming spikes. Therefore, when the activity in the presynaptic cell switches from a low rate to a maintained high rate, the postsynaptic conductance might increase strongly with the initial rate change, but then decay back towards the value it had before the change¹⁰. We will simulate such effects in Tutorial 5.1.

Mathematically, synaptic depression produces negative feedback, as the greater the firing rate the lower the synaptic efficacy. Negative feedback is a method for control of circuit activity, as by limiting the amount of synaptic transmission, the possibility of runaway feedback excitation is reduced. Synaptic depression also causes adaptation to ongoing inputs. Adaptation, which we have seen in the spike-rates of neurons (Figures 2.7-2.8), is important in sensory systems, allowing us to perceive changes in inputs without being swamped by background levels.

5.3.2. Short-term synaptic facilitation

Synaptic facilitation provides a counterpoint to synaptic depression as it increases synaptic efficacy immediately after a presynaptic spike. Synaptic facilitation corresponds to a temporary increase in the release probability of those vesicles that remain docked in the membrane of the axon terminal following a spike. Release-ready vesicles may be bound by some but not all of the proteins necessary for release of neurotransmitter following an action potential. If a second action potential follows soon on the heels of the first, those proteins may still be binding the vesicle, making it much more likely for all the necessary steps to be completed for neurotransmitter release. Residual calcium in the presynaptic terminal also enhances release probability⁹. The timescale over which facilitation persists depends on the rates of dissociation of those proteins and return of calcium to baseline levels. In most observations, the longest time constant is about a half-second, but time scales of several seconds have been observed and used in models^{9,11}.

Synaptic facilitation is a positive feedback process—the more rapidly spikes arrive at the axon terminal the more likely any remaining vesicles will release neurotransmitter, so the greater the synaptic efficacy. The positive feedback can allow the postsynaptic cell to remain insensitive to any low-rate spontaneous activity of a presynaptic cell ('noise') while producing very strong responses to higher firing rates or a burst of presynaptic activity ('the signal').

Synaptic facilitation can dominate over synaptic depression when initial release probability is low. For such a synapse, the fraction of vesicles lost after an initial spike is low, so synaptic depression is not strong—most vesicles still remain for the next spike. Moreover, if the initial release probability is low, it has a lot of 'room' to increase toward one for a subsequent spike. Conversely, if the release probability is nearly one for an initial spike, it cannot increase further for a subsequent spike and facilitation is not possible, yet depression would be strong.

5.3.3. Modeling dynamical synapses

The expected number of vesicles releasing neurotransmitter following an action potential is the number of docked, release-ready vesicles multiplied by their individual probability of release. The first number is affected by synaptic depression, the second by synaptic facilitation, so we can simply multiply the two effects together to obtain the synaptic efficacy at any time^{7,8}.

We let D be the variable for synaptic depression ($0 \leq D \leq 1$) denoting the fraction of docked release-ready vesicles compared to the number it attains after quiescence. We let F be the variable for synaptic facilitation ($1 \leq F \leq F_{max}$) such that the release probability at any point in time is $p_0 F$, where p_0 is the initial release probability. Note that $F_{max} = 1/p_0$ since the maximum release probability is one. By combining these terms, we find the change in synaptic conductance following a spike is given by:

$$\Delta G = G_{max} p_0 F D. \quad \text{Eq. 5.8}$$

Both the depression and facilitation variables return to the value of one in between spikes, so follow equations of the same form,

$$\frac{dD}{dt} = \frac{1 - D}{\tau_D}, \quad \text{Eq. 5.9a}$$

and

$$\frac{dF}{dt} = \frac{1 - F}{\tau_F} \quad \text{Eq. 5.9b}$$

which produce decaying exponentials between spikes. A qualitative difference arises between Eq. 5.9a and Eq. 5.9b, because D increases to 1 from lower values, while F decreases to one from higher values. Following each spike the values of F and D are updated via:

$$D \mapsto D - p_0 FD \quad \text{and} \quad F \mapsto F + f_{fac}(F_{max} - F). \quad \text{Eq. 5.10}$$

The first update reduces D by the fraction of vesicles emptied during the spike.

Notice that we are taking the mean here, a quantity which may not be valid for a particular synapse—for example if a synapse has 5 vesicles with a release probability of $p_0 F = 0.5$, this equation suggests 2.5 vesicles are released. Such a result is fine if we assume we are averaging over many synapses. However, when individual synapses are simulated independently then, in a much more computationally intensive procedure, the Binomial distribution must be sampled for each synapse to produce probabilistically, the integer number of vesicles released. For such a simulation, a variable indicating the state of each synapse must be stored. Instead here, we just need a single variable to represent the mean state of synapses of the presynaptic cell.

The second update increases the facilitation variable towards its maximum by a factor f_{fac} that denotes the degree of facilitation ($0 \leq f_{fac} \leq 1$). If f_{fac} is zero, there is no facilitation, while if f_{fac} is one then a single presynaptic spike causes the release probability to jump to one immediately thereafter. In practice, those synapses with the most facilitation never have an increase in release probability of more than 4 following a spike. This limits the valid values of f_{fac} to be less than $\frac{3p_0}{1-p_0}$ for $p_0 \leq \frac{1}{4}$ to ensure $F \leq 4$, and $f_{fac} \leq 1$ for $p_0 \geq \frac{1}{4}$ so that $F \leq F_{max}$ and release probability is never greater than one.

5.4. Tutorial 5.1. Synaptic responses to changes in inputs

Neuroscience goals: Understand the contrasting effects of synaptic depression and facilitation on the steady-state and transient responses of synapses to changes in presynaptic rates.

Computational goals: More practice with a time-varying Poisson process; combining multiple variables with step-wise changes and continuous variation in coupled ODEs.

In this computer tutorial, you will treat the spike train of a presynaptic neuron as a Poisson process whose emission rate will change step-wise at discrete times. You will examine the synaptic response to these inputs first in a synapse without short-term changes in efficacy, second in a synapse with synaptic depression, and finally in a synapse with synaptic facilitation. If time permits you will simulate the response of a postsynaptic LIF cell to these inputs. This tutorial is based on Figure 5.19 of the textbook by Dayan and Abbott¹².

- Produce a time-vector, with time-steps of size $\delta t = 0.1\text{ms}$, from 0 to 4 seconds.
- Produce a vector of the same size as the time vector with presynaptic firing rates of 20Hz, 100Hz, 10Hz, and 50Hz for each one-second portion of the time period.
- Produce an array of ones and zeros to represent a Poisson spike train (Section 3.3.3), such that the probability of a spike in any time-bin of size δt is equal to $\delta t \times r(t)$ where $r(t)$ is the firing rate at that time-bin generated in b) (you can ignore the possibility of multiple spikes in a time-bin).

- d) Produce a synaptic conductance vector, $G_{syn}(t)$, which increments by $\Delta G = 1nS$ when each spike arrives and decays back to zero between spikes with a time constant of 100ms. Plot $G_{syn}(t)$ versus time.
- e) Assume an initial release probability of $p_0 = 0.5$ and produce a synaptic depression vector, $D(t)$, that is initialized to one, decreases by an amount $p_0 D(t)$ following each spike at time, t , and recovers via $\frac{dD(t)}{dt} = \frac{1-D(t)}{\tau_D}$ with time constant of $\tau_D = 0.25s$.
- f) Produce a second synaptic conductance vector with decay time constant of 100ms that increments by $\Delta G = \Delta G_{max} p_0 D(t_-)$ following each spike at time, t , where $\Delta G_{max} = 5nS$, $p_0 = 0.5$, and where $D(t)$ is obtained from e). The symbol t_- is to indicate the time immediately preceding the spike, so that you use the value of $D(t)$ calculated just before its decrease due to that spike. Plot the conductance versus time.
- g) Assume an initial release probability of $p_0 = 0.2$ and produce a synaptic facilitation vector, $F(t)$, that is initialized to one, increases by an amount $f_{fac}(F_{max} - F(t_-))$ following each spike at time, t , and recovers via $\frac{dF(t)}{dt} = \frac{1-F(t)}{\tau_F}$ with time constant of $\tau_F = 0.25s$, facilitation factor, $f_{fac} = 0.25$, and maximum facilitation of $F_{max} = 1/p_0$.
- h) Produce a new synaptic depression vector initialized to one, which decreases by an amount $p_0 F(t_-) D(t_-)$ following each spike at time, t , and which recovers as in e), with $p_0 = 0.2$ and $F(t)$ generated in g).
- i) Produce a third synaptic conductance vector with decay time constant of 100ms that increments by $\Delta G = \Delta G_{max} p_0 F(t_-) D(t_-)$ following each spike at time, t , where $\Delta G_{max} = 4nS$, $p_0 = 0.2$, $F(t)$ is obtained from g), and $D(t)$ is obtained from h). Plot the conductance versus time.

Comment

100ms is a long synaptic time constant but necessary in this simplified model to see accumulation of inputs from a single spike train. To observe such accumulation, we have assumed that the postsynaptic receptors are never completely saturated by neurotransmitter. However, this is unlikely when neurotransmitter is released at a high rate and the time constant for dissociation and closing of channels is as high as 100ms. To include the effects of such saturation the update term should be replaced, for example in i), by $\Delta G = (G_{max} - G_{syn}) p_0 F(t_-) D(t_-)$, with $G_{max} = 4nS$.

Alternatively, we can assume that a time-varying stimulus impacts a neuron via multiple synaptic inputs. In Option A we will simulate 50 such inputs via synapses with a 2ms time constant—a short enough synaptic decay time that saturation can be neglected.

Optional Problems

OPTION A

- j) Initialize a new total conductance vector of the same size as the time vector. Using a “for” loop, repeat c) – d) 50 times (once each for each of the 50 inputs) each time using a new Poisson spike train. Make the alteration of a 2ms time constant for decay of synaptic conductance. Within the loop accumulate the total conductance at each point in time by summing across the values generated for that time point by

- each of the 50 input vectors. Plot the summed vector and compare it to the one plotted in d).
- k) Repeat j), but use synaptic depression—with a separate value for each input—while using all other variables as in e) and f). Compare the summed conductance vector to the one plotted in f).

OPTION B

- l) Simulate the postsynaptic cell as a leaky integrate-and-fire neuron with parameters $E_L = -65\text{mV}$, $E_{syn} = 0\text{mV}$, $G_L = 2\text{nS}$, $C_m = 20\text{pF}$. The model neuron will receive inputs $G_{syn}(t)$ given by each result produced above in d), f), and i). In this example, E_{syn} is the reversal potential of an excitatory synapse. (If the synapse were inhibitory, we would use a value for E_{syn} in the region of E_L .) Use the equation

$$C_m \frac{dV}{dt} = G_L(E_L - V) + G_{syn}(t)(E_{syn} - V)$$

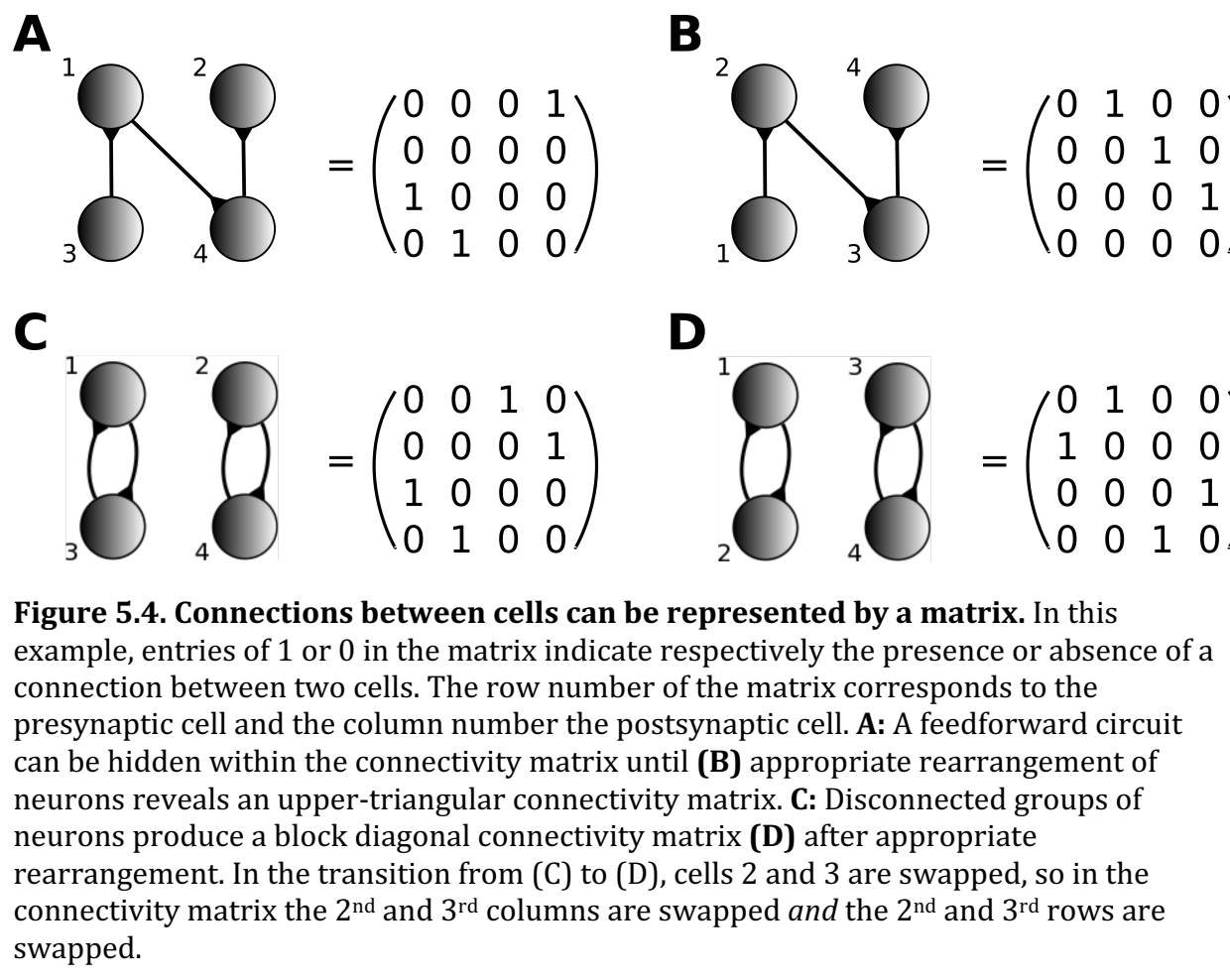
to simulate the membrane potential, V , which produces a spike whenever it crosses a threshold given by $V_{th} = -50\text{mV}$, after which it is immediately reset to $V_{reset} = -80\text{mV}$. Plot V versus t and count the number of spikes produced in the four intervals of distinct input firing rate, commenting on how the numbers differ across the three types of synapse.

5.5. The connectivity matrix

A remarkable property of neurons that distinguishes them from other cells is their physical structure. Dendrites and axons of a neuron can extend far from the cell body, ramify to generate hundreds of branches with thousands of possible connection points, and target specific regions and sub-regions or layers of the brain, producing contacts with a highly selective subset of other cells. In most models of neural circuits—including those produced in this course—all of the spatial intricacy and important cell biology needed to produce such extensive architectures is subsumed into a connectivity matrix, which simply tells us whether any two neurons are connected and ignores their actual position within the physical space of the brain.

Box 5.21. Connectivity matrix: A square matrix indicating the absence or presence, the direction, and sometimes the strength, of all connections within a group of neurons.

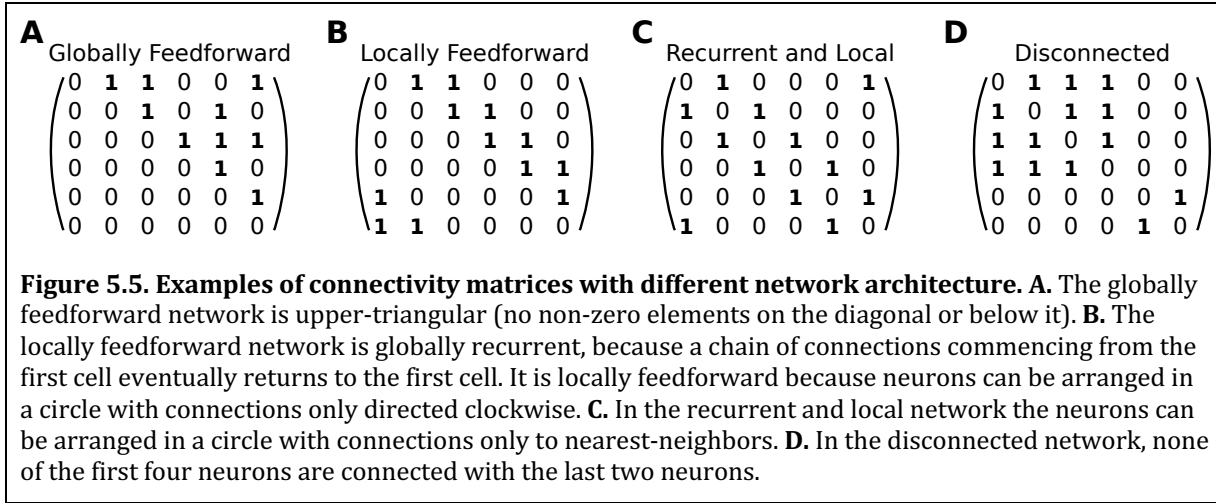
One concession to the reality of physical space in some models is the inclusion of a delay from spike generation in the soma to the time of synaptic transmission, or from the time of EPSC in a dendrite to current flow in the soma. Multi-compartmental models can and do include more realistic consequences of the physical dimension for each cell. As more data is accrued, not only of which cells are connected, but also where those connections occur relative to the cell body, such features can be incorporated into circuit models.



In this course, any model of a neural circuit is simulated with point neurons, so all that is needed is a single number to indicate the presence and strength of any connection, between each pair of neurons. The connectivity of an entire circuit can then be represented as a matrix of size $N \times N$ where N is the number of neurons. See Section 1.4.2 for an introduction to the use of matrices if necessary.

Connectivity matrices can be defined at multiple scales. For a circuit containing a small number of neurons, each entry in the connectivity matrix represents a directed connection from one neuron to another—a single entry could represent multiple connections between the same presynaptic and postsynaptic cells. In models of larger circuits and networks, each entry can represent the effect of one functional unit on another, where a functional unit comprises a group of cells with similar responses to stimuli—for example, similar receptive fields in sensory areas. The average activity of such groups acting as functional units is considered via firing rate models in Chapter 6. At the largest scale of whole human brain models, each element in the connectivity matrix corresponds to the connection or correlation between discrete volumes of brain tissue. Examples of such large-scale connectivity matrices include the functional connectivity based on correlated activity between regions acquired by functional magnetic resonance imaging (fMRI), and structural connectivity based on magnetic resonance imaging of fluid flow combined with

tensor analysis (the whole process known as diffusive tensor imaging, DTI). In this section, we focus on connections at the level of individual neurons.



If we write W_{ij} as the strength of connection from neuron i to neuron j then each row of the matrix corresponds to a single presynaptic cell and each column corresponds to a single postsynaptic cell. Since synaptic connections are directional, a synapse from neuron i to neuron j can be present without a synapse from j to i . This means the matrix W_{ij} is not symmetric and rows cannot be switched with columns—so one must be careful about which (of rows or columns) correspond to presynaptic cells and which correspond to postsynaptic cells.

The effect of a connection is determined not by a single number—its strength—but also by other synaptic properties. In particular, given differences in the reversal potential, one needs separate connectivity matrices for inhibitory connections when simulating synaptic input as a change in conductance. However, in simpler models, synaptic input can be simulated as a current and it is possible to use a single matrix with negative entries for inhibitory connections. The negative entry corresponds to the amount of negative current that can be produced by inhibitory synaptic input. Dale's Principle could then be observed by ensuring each row of the matrix only contains positive entries for an excitatory presynaptic cell and only negative entries for an inhibitory presynaptic cell.

5.5.1. General types of connectivity matrices

The diagonal entries of a connectivity matrix correspond to self-connections or autapses, which are uncommon in practice (an exception being for fast-spiking inhibitory neurons)¹³. Thus, diagonal entries are usually zero for connectivity matrices representing individual neurons. This is in contrast to connections between units or groups of similar cells, in which case connections within a group can be the strongest, leading to diagonal entries of the connectivity matrix being the largest.

It can be daunting to observe structure within a connectivity matrix of more than a few neurons. When there is underlying structure it can be made more apparent by appropriate ordering of the neurons. If two rows of a connectivity matrix are switched with each other and the corresponding two columns are switched, then the connections

represented by the matrix are unchanged—only the labels of two of the neurons have been switched with each other (Figure 5.4). In Tutorial 5.2 we will see how structure can be made clearer within the connectivity matrix by appropriate ordering of the rows and columns.

Some particular terms for features of a connectivity matrix are described below:

Sparse: most possible connections are absent, so most entries of the matrix are zero.

Globally feedforward: neurons can be ordered with no connection from a later neuron to an earlier one in the order. The matrix can be transformed to be upper-triangular (Figure 5.5A).

Locally feedforward: a recurrent network can be locally feedforward if neurons connect to neurons without a reciprocal connection, but may receive inputs from neurons that are a few connections downstream, so the architecture is one of a loop with a particular direction of information flow or activation around the loop (Figure 5.5B).

Recurrent: neurons receiving input from a cell can influence that cell in return, either by a direct connection or via connections to other cells (Figure 5.5C).

Disconnected: some sets of neurons neither receive input nor provide input to other sets. In such a case the connectivity matrix can be rearranged into a block diagonal form (Figure 5.5D).

Clustered: the neurons can be arranged into groups with significantly stronger connections or greater proportion of connections within a group than between groups.

Local: neurons can be labeled with indices such that neurons with similar indices are more likely to be connected than neurons with very different indices. If the indices are spatial coordinates then local connectivity is local in space, so connections are spatially structured (Figure 5.5C).

Small world: any neuron can reach any other neuron via a small number of connections and neurons that are connected with each other connect with a highly overlapping group of other neurons. Clustered networks can be small world networks.

5.5.2. Cortical connections—sparseness and structure

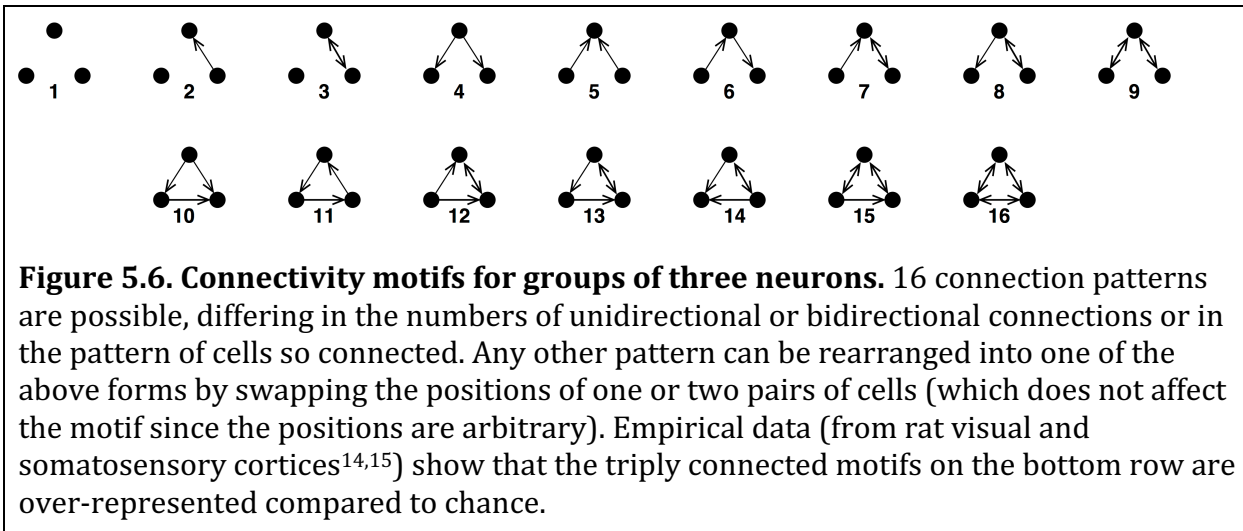
Within cortical circuits the connections are sparse—even cells whose dendrites and axons intertwine connect with only 10-20% likelihood. The probability that any two cells are connected increases with the number of other cells with which they have connections in common. Another way of putting this, is that if two cells are connected, the two sets of other cells to which they each connect have more overlapping members than is expected by chance. Furthermore, if any two cells respond similarly to stimuli, they are more likely to be connected than is expected by chance. Such connectivity features can arise via correlational learning (Hebbian learning), which we will discuss in Chapter 8 and can be summarized as “connections preferentially strengthen and remain intact between pairs of neurons that are active at the same time”.

5.5.3. Motifs

When the presence or absence of connections between all pairs of cells in a group is known, then various motifs can be enumerated and compared to chance or to predictions of models. Motifs represent all the distinct ways in which a small group of cells can be interconnected and are best considered visually. The simplest motifs are for two cells, which can be disconnected, or unidirectionally connected, or bidirectionally connected,

producing three possible motifs. For a group of three cells of the same type, there are in fact 16 distinct possible motifs (shown in Figure 5.6).

Box 5.22. Motif: The representation of a pattern of connections within a group of cells, with connections depicted as lines or arrows (edges) and the cells as points (nodes).



When considering the abundance of different motifs, one should consider first what would be expected a priori from random connections, and then what would be produced by different types of connectivity matrix. Also, when measuring these connectivity patterns in real tissue, it is important first to account for spatial location of cells—if two cells are far apart then the likelihood they are connected is lower than if they are nearby, simply because axons and dendrites have limited ranges over which they are highly branched with a high density of potential contacts. The decrease in connection probability with spatial separation leads to an abundance of the highly-connected motifs (*e.g.* motifs 12–16 in Figure 5.6) compared to chance if the circuit being characterized spreads over a wide range of space. That is because if two cells are connected they are more likely to be near each other and both cells are more likely to connect to a third nearby cell than to other cells on average. Such factors mean that motifs are often measured only within local circuits where all of the cells have the potential to be highly interconnected.

However, one benefit of the computational approach advocated in this book, is that the effects of confounding features observed in experiments can be simulated and accounted for. In this case, spatial structure can be controlled for by comparison with simulated connectivity matrices that incorporate the observed separation-dependence of connection probability. Thus, one could assess whether particular motifs observed in brain tissue are overabundant in excess of what is expected from the spatial distribution of cells—and observed in simulated circuits. Moreover, the simulated circuits allow one to extract statistical significance, simply by enumerating the fraction of, say 1000 different random instantiations of a circuit, that contain a particular motif with the observed abundance or greater.

Tutorial 5.2 provides experience in generating different types of connectivity matrix and analyzing a matrix for structure that might be hidden. Observing structure in a connectivity matrix is not always easy until the neurons have been ordered appropriately. Even a network containing two entirely disconnected circuits might not appear as such from a glance at the connectivity matrix if the number of cells is high (Figure 5.7). Therefore, a major goal of Tutorial 5.2 is to introduce you to routines that switch around the labels of connections to allow easy extraction then visualization of any underlying structure.

A	B
$ \begin{matrix} & a & b & c & d & e & f & g & h & i \\ a & \begin{pmatrix} 1 & 0 & 0 & 0 & 1 & 0 & 0 & 0 & 1 \\ 0 & 0 & 1 & 1 & 0 & 0 & 1 & 0 & 0 \\ 0 & 0 & 0 & 1 & 1 & 0 & 0 & 0 & 0 \\ 0 & 1 & 1 & 0 & 0 & 0 & 1 & 0 & 0 \\ 1 & 0 & 0 & 0 & 0 & 1 & 0 & 0 & 1 \\ 0 & 0 & 0 & 0 & 1 & 1 & 0 & 1 & 0 \\ 0 & 0 & 0 & 1 & 0 & 0 & 1 & 0 & 0 \\ 1 & 0 & 0 & 0 & 1 & 0 & 0 & 1 & 0 \\ 0 & 0 & 0 & 0 & 1 & 1 & 0 & 0 & 1 \end{pmatrix} \end{matrix} $	$ \begin{matrix} & a & e & f & h & i & b & c & d & g \\ a & \begin{pmatrix} 1 & 1 & 0 & 0 & 1 & 0 & 0 & 0 & 0 \\ 1 & 0 & 1 & 0 & 1 & 0 & 0 & 0 & 0 \\ 0 & 0 & 1 & 1 & 0 & 0 & 0 & 0 & 0 \\ 1 & 0 & 1 & 1 & 0 & 0 & 0 & 0 & 0 \\ 0 & 1 & 1 & 0 & 1 & 0 & 0 & 0 & 0 \\ 0 & 0 & 0 & 0 & 0 & 1 & 1 & 1 & 1 \\ 0 & 0 & 0 & 0 & 0 & 0 & 1 & 1 & 0 \\ 0 & 0 & 0 & 0 & 0 & 0 & 0 & 1 & 1 \\ 0 & 0 & 0 & 0 & 0 & 0 & 1 & 0 & 1 \end{pmatrix} \end{matrix} $

Figure 5.7. Hidden structure revealed by rearranging labels. The connectivity matrix in **(A)** contains two disconnected recurrent circuits that can be revealed by reordering the cells as shown in **(B)**. The resulting matrix is block-diagonal, meaning that entries are zero apart from specific squares along the diagonal, in this case a 5x5 square then a 4x4 square. The two matrices correspond to identical circuit structure, but the particular ordering on the right makes it easier for us to visualize such underlying structure.

5.6. Tutorial 5.2. Detecting circuit structure and non-random features within a connectivity matrix.

*Neuroscience goals: acquire techniques that are useful in the analysis of connectivity data.
Computational goals: gain experience at manipulating, sorting, and shuffling rows or columns of matrices; use of the “while” loop.*

In this tutorial, you will produce a connectivity matrix with structure that is not clear by inspection of the matrix. You will write an algorithm to extract the “hidden” structure and to analyze it for motifs that are present at levels significantly above chance.

PART A

1. Create a vector of length N_{cells} , where $N_{cells} = 60$, such that each element of the vector is a random integer from 1 to 4. This vector indicates the group to which each cell belongs. (Hint, either use the numpy functions “ceil” and “random.rand” or the single function “random.randint” to achieve this.)
2. Create a connection matrix, C , of size $N_{cells} \times N_{cells}$, where each element, C_{ij} , representing the presence or not of a connection from neuron i to neuron j , is 1 or 0.

Let $C_{ij} = 1$ with a probability of $p_0 = 0.1$ if neurons i and j belong to different groups and with a probability of $p_1 = 0.5$ if neurons i and j belong to the same group. *Hint:* It is efficient to create a matrix of size $N_{cells} \times N_{cells}$ with each element a random number between 0 and 1 using numpy's "random.rand" function then set all random values less than the probability to a 1 and all random values greater than the connection probability to a 0.

3. Plot the connection matrix in 2D (*e.g.*, using the matplotlib function "imshow").

PART B

The goal is to rearrange the neurons into their respective groups so that the structure of the connection matrix can be made visible.

4. To begin, you will create two correlation matrices, one set of correlations between all the outgoing connections of all cells, the other set of correlations between all the incoming connections of all cells. The expectation is that if two cells belong to the same group their connections will be more strongly correlated than between two cells of different groups.
 b) Calculate the correlation matrix for outgoing connections by evaluating the correlations between all pairs of row vectors of \mathbf{C} . The correlation matrix so produced will be of size $N_{cells} \times N_{cells}$ (with a diagonal of 1, because each row is perfectly correlated with itself).
 c) Repeat b) for all pairs of column vectors of \mathbf{C} to evaluate the correlation matrix between all incoming connections of cells.
 d) Sum the two correlation matrices to produce a matrix called `total_corr` and plot the histogram of values. (If it is bimodal, that is a good sign of clustering).
5. We wish to set a threshold for the correlation between two cells such that if the correlation is above the threshold we will ascribe the same group identity to those two cells. The number of resulting groups will depend on the threshold—if it is set too low then only one group will be found, whereas if it is set too high many groups might be found. Select a threshold such that 10% of all correlations are above the threshold (one method is to use the numpy function "sort" without an axis:
`np.sort(total_corr, axis=None)`).

Alternative Simplification: just choose a threshold of 0.5 and adjust it up or down to obtain the correct number of groups after running the code if necessary.

6. To begin assigning cells to groups, create a vector of zeros that will contain the group identity of each cell (this will be the discovered identities, not the known ones generated in part 1). Set a new variable to zero—this variable will act as a group counter. Create a "for" loop so that a variable, i , runs through all N_{cells} .
7. Within the loop check the currently assigned group identity of cell number i , with an "if" statement—if the group identity is zero (as it will be initially, when $i=0$) then increase the group count by one to commence extraction of a new group. Do parts 8-10 within the "if" statement (*i.e.*, only if group identity of the cell reached was zero, meaning it has not yet been allocated to a group). If the currently assigned group identity is above zero, it means this cell has been found within a completed cell-group, so just increase i by 1 and test whether the next cell requires a new group.

The goal of these next three parts is to ascertain which other cells are in the same group as cell number i . This requires finding which cells have an above-threshold correlation with cell i , which other cells have an above-threshold correlation with these, and so on until no more new cells are found in the group. Have a go at doing this yourself if you are confident, without following the instructions in parts 8-.

8. Initialize two vectors, one containing cells in the group whose high-correlation partners remain to be found (a “remaining” list), the other which will contain the cells in the group whose high-correlation partners are already found (a “used” list). The first vector is initialized with the single element i , while the second vector is initialized as the empty vector “[]”.
9. Create a loop using a “while” statement, which will continue until the list of remaining cells is empty. Once the list of remaining cells is empty, the code should go to the next step of the “for” loop and increment i by one.
 - a. Within the “while” loop extract the neuron that is the first element of the list of remaining cells.
 - b. Then find all cells with correlation greater than the threshold with this neuron.
 - c. Give the current group identity to all of those cells (in so doing you will give the group identity to the neuron being used as its self-correlation is 1, so is certainly above-threshold).
 - d. Add the current neuron to the “used” list then add the group of cells just found to the “remaining” list.
 - e. Remove all double counts on the “remaining” list, so each cell on it appears only once. Then remove from the “remaining” list any cell that is on the “used” list. This is to ensure that we avoid an endless loop where we keep looking for high-correlation partners of the same set of cells over and over. A danger of “while” loops is that they might never end!
10. End the “for” loop begun in step 6, so that the code returns to step 7 with the cell number i increased by 1.
11. After the “for” loop in i has completed, use the “sort” command to sort the list of group identities—be sure to store the indices such that alongside the sorted list of group identities is the list of cells to which the group identities belong. Produce and plot an alternative connection matrix with the entries reordered according to the sorted list of group identities to observe the underlying group structure.

OPTIONAL: PART C

Our goal is to extract motifs and compare their abundance with what one expects by chance given the average connection probability.

12. Find the average connection probability, \bar{p} , between pairs of cells in the original connection matrix.
13. Find the number of cell-pairs with bidirectional connections and compare the number with what is expected by chance, given your answer in 12.
14. Use your answers to questions 12 and 13 to calculate the probability of a cell-pair having two connections, p_2 , a single connection, p_1 , or no connection, p_0 . Hint: total

number of connections must be $N_{pairs}\bar{p} = N_{pairs}p_1 + 2N_{pairs}p_2$, where $N_{pairs} = N_{cells}(N_{cells} - 1)/2$ is the total number of cell-pairs.

15. Look at the motifs in Figure 5.6 and enumerate the number of each type found in the connectivity matrix. For example: initialize a vector of length 16 with zeros; using three nested loops running from 1 to N_{cells} for variables i , j (with $j > i$), and k (with $k > j$), test each triplet of connections, and add 1 to the count of the corresponding motif number.
16. To compare with chance, plot the ratio of counts enumerated in Q.14 with the expected number, E_i , for motif i , obtained from the following formula:

$$E_i = M(i)N_{triplets}p_0^{n_0(i)}p_1^{n_1(i)}p_2^{n_2(i)}$$

where $n_0(i)$, $n_1(i)$, $n_2(i)$ are the numbers of unconnected, unidirectionally connected and bidirectionally connected cells in the motif, $N_{triplets} = N_{cells}(N_{cells} - 1)(N_{cells} - 2)/6$ is the number of distinct cell-triplets, and $M(i)$ is the number of ways of producing the motif by shuffling connections between the cells, as given in Table 5.1. Note that the sum of multiplicities in Table 5.1 is $2^6 = 64$, the total number of patterns given the 6 possible connections, each of which is either absent or present, between 3 cells.

Motif label	1	2	3	4	5	6	7	8	9	10	11	12	13	14	15	16
Multiplicity	1	6	3	3	3	6	6	6	3	6	2	3	6	3	6	1

Table 5.1. For each 3-neuron motif (Figure 5.6), the number of distinct sets of connections between the three cells that produce the same motif is given as the multiplicity.

5.7. Oscillations and multistability in small circuits.

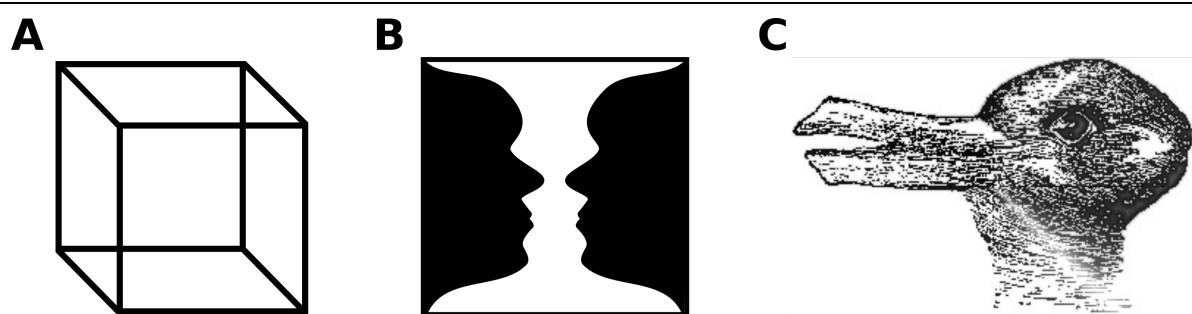


Figure 5.8. Images producing bistable percepts. **A)** The Necker cube can be seen with its front face as bottom-right or top-left. The 3D percept produced by such a 2D line-drawing is experience-dependent—a 50-year old who gained sight after being blind from birth did not perceive a cube. We will consider how experience-dependent synaptic strengthening can produce multistable circuits in Chapter 8. **B)** Rubin's vase can appear as a single white vase in the center or two black faces looking at each other (first created by the Danish psychologist Edgar Rubin in 1915¹⁶). **C)** The image by Joseph Jastrow in 1899¹⁷ can appear either as a leftward facing duck or a rightward facing rabbit.

The response of a neural circuit depends not only on the external inputs it receives but, perhaps more so, on the internal connections within the circuit.

Once neurons are connected with each other they can exhibit patterns of activity that are not present in the individual disconnected neurons. We have seen that many single neurons oscillate, either with a single sodium spike per cycle, or with a burst of sodium spikes riding on a slower calcium spike. Neurons that do not oscillate alone can oscillate when connected to other neurons, in particular if there is inhibitory feedback.

Alternatively, a system with more than one stable state can result from the connections between cells, the simplest example being a “flip-flop”, a bistable switch in which one of two neurons, or groups of neurons, suppresses the other. The behavior of such small circuits can depend subtly on attributes of the synaptic connections, such as their strengths, time constants, and whether short-term depression or facilitation dominate, as well as on the intrinsic properties of each cell.

Box 5.23. Multistability: The existence of more than one stable pattern of activity or stable level of activity in a system in response to a particular set of inputs.

Box 5.24. Quasistable: A system that reaches a state that is almost stable, but, perhaps due to a slowly varying property, eventually changes away from that state.

The simplest form of multistability is bistability, meaning that under constant stimulus conditions two states of neural activity are possible. A widely-appreciated phenomenon in the fields of vision and psychology is perceptual bistability, whereby a single image can appear as one of two possible objects or scenes. Some examples of images giving rise to bistable percepts are shown in Figure 5.8. If an observer fixes her eyes on the image then occasional transitions from one percept to the other are common. It should be noted that mathematically, if the percept does switch at regular intervals then the system is an oscillator and not bistable (a state is not stable if it does not persist). In Tutorial 5.3 we will see the close relationship between bistable systems and oscillators. Oscillators that are based on regular switching between states that are almost stable (quasistable) are called relaxation oscillators (Section 7.6).

5.8. Central Pattern Generators

A central pattern generator is a neural circuit that can produce, autonomously, a pattern of activity, such as an oscillation, which can drive muscles in a reliable manner¹⁹. While external input can switch the central pattern generator on or off, or switch it between modes, and neuromodulation can adjust features of the pattern, the neural circuit of a central pattern generator does not rely on any external input to produce the activity pattern. The oscillator in Part B of Tutorial 5.3 (Figure 5.9A) is a simple example of a central pattern generator, related to that found in the heart-beat control system of the medicinal leech^{18,20}. Whenever animals have stereotypical coordinated muscle contractions accompanying a behavior—such as breathing, peristalsis, locomotion, or chewing—central pattern generators are typically involved.

The most important goal of a central pattern generator is to ensure the muscles contract in the correct order. This requires that the neurons in the circuit are active in a

regular, predictable order. The connectivity pattern between neurons can determine the order of activation of cells. When it is essential that different muscles do not contract at the same time, then cross-inhibition between the neurons controlling those muscles is a solution²¹. Thus, in the two examples we consider here, the rhythms are produced by inhibitory cross-connections.

Two other characteristics of a central pattern generator that should be controlled are the frequency of oscillation (or duration if non-oscillating) and the duty cycle of each neuron, that is the relative time it spends active versus quiescent. In many cases in nature, the frequency of oscillation can vary in response to external conditions or internal control, without any change in the order of firing and the duty cycles of the neurons involved. It is far from trivial for us to produce models of central pattern generators with such properties²², but biological evolution often achieves solutions that we might not think of.

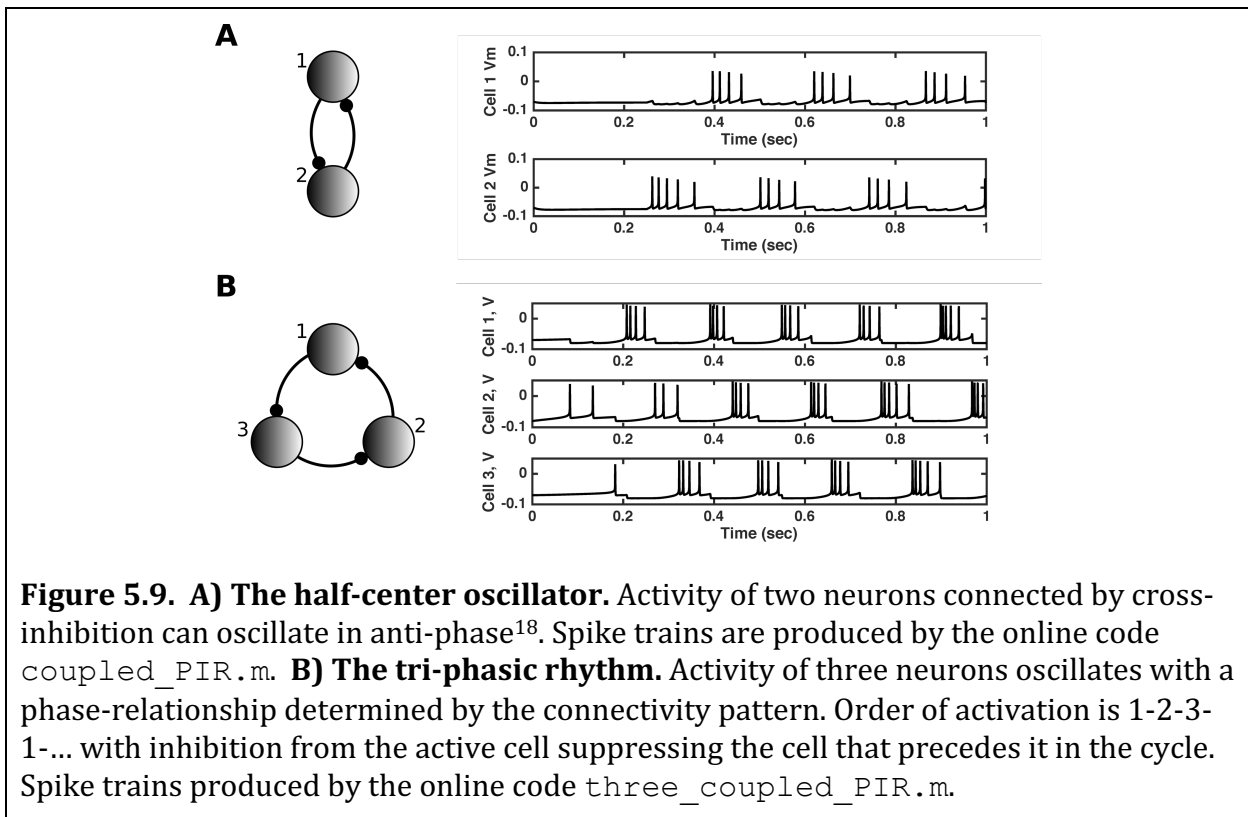


Figure 5.9. A) The half-center oscillator. Activity of two neurons connected by cross-inhibition can oscillate in anti-phase¹⁸. Spike trains are produced by the online code `coupled_PIR.m`. **B) The tri-phasic rhythm.** Activity of three neurons oscillates with a phase-relationship determined by the connectivity pattern. Order of activation is 1-2-3-1-... with inhibition from the active cell suppressing the cell that precedes it in the cycle. Spike trains produced by the online code `three_coupled_PIR.m`.

5.8.1. The half-center oscillator

The half-center oscillator (Figure 5.9A) is achieved with two neurons, each of which inhibits the other. Each neuron's activity oscillates in antiphase with the other, so the neurons can produce muscle contractions that alternate between two antagonistic muscles. Such alternating contractions between the two sides of an animal's body comprise the basic unit for locomotion by slithering or wiggling, most common among long leg-less animals (lampreys, eels, snakes, worms etc.)²³. It appears that evolution has ensured the neural circuits are wired, not only to produce the individual half-center oscillators that comprise the basic units, but also to ensure the correct phase relationship between successive units that is necessary to produce effective motion²⁴.

The frequency of a half-center oscillator depends on the time from when one of the neurons commences its activity until the other one takes over. The switch in the dominating neuron can occur either because the active neuron cannot sustain high activity for very long or because, following suppression, the inactive neuron becomes more excitable over time. The first mechanism for switching is called *release* and the second is called *escape*¹⁸.

Release is so-called, because as the activity of the active neuron decreases, so the inhibitory input to the inactive neuron decays away. Such weakening and eventual loss of inhibition from the active cell is the release. The period of the oscillation is dominated by the timescale of inactivation of the active cell.

Switching by escape depends on a regenerative process, such as deinactivation of an excitatory current, within the inhibited neuron. The time for the inhibited neuron to overcome the inhibition and become active again depends strongly on the strength of the inhibitory connection, but also the strength and timescale of the regenerative process.

5.8.2. *The tri-phasic rhythm*

The simplest models of a tri-phasic rhythm require three neurons, which activate in a reliable cyclic order (Figure 5.9B). As with the half-centered oscillator, the rhythm can be produced with inhibitory connections alone, if each cell can fire spontaneously or via post-inhibitory rebound. In this case, the inhibition of one neuron suppresses the activity of the neuron preceding it in the cycle. The time for a neuron to rebound from such inhibition is a key determinant of the oscillation frequency.

The best-studied tri-phasic rhythm is the pyloric rhythm produced in the stomatogastric ganglion of the lobster or crab. The rhythm controls stomach contractions and dilations. Although the numbers and types of cells and their connectivity pattern are conserved across individuals of any species, the synaptic connection strengths and values of intrinsic cell conductances vary over wide ranges across individuals. An intriguing question is how, in spite of the huge individual variation, the important characteristics of the rhythm are maintained—in particular, because in models, if any one parameter is varied to the degree observed in nature, then the rhythm produced by the circuit changes dramatically or disappears.

5.8.3. *Phase response curves*

A useful technique for understanding the behavior of coupled oscillators is analysis of their phase response curves²⁵. A phase response curve (Figure 5.10) indicates how an oscillator responds to a perturbation, such as a brief excitatory synaptic input. The phase response is quantified by the amount of advancement or delay of ensuing oscillations caused by the perturbation. The response can depend on the point in a cycle at which the perturbation occurred.

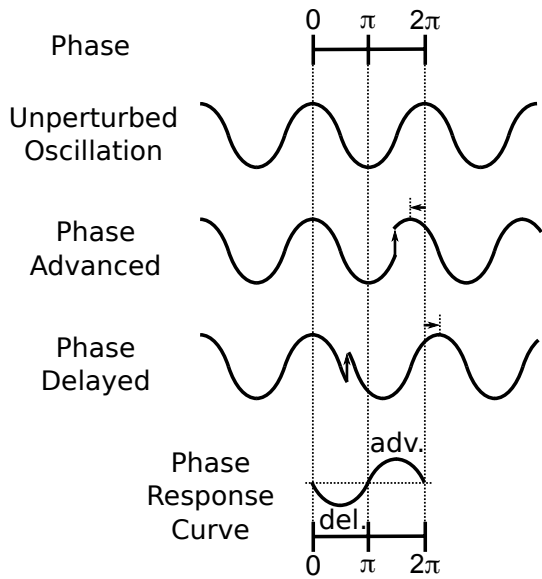


Figure 5.10. The phase response curve (PRC). A phase response curve can be produced for any system undergoing periodic activity—*i.e.*, an oscillator (**top**)—such as a regularly spiking or bursting neuron. If the oscillator is perturbed by an input, such as a brief pulse of excitation (vertical arrow), it can be advanced in phase (a positive phase response, **upper curve**) or delayed in phase (a negative phase response, **lower curve**). The phase response curve (**bottom**) is produced by measuring the change in phase (horizontal arrows) as a function of the point in the cycle at which the perturbation arises. Regularly bursting and Type-II neural oscillators typically have biphasic phase response curves similar to the one sketched here.

Box 5.25. Perturbation:

A small, externally produced, change in a system.

For example, a brief pulse of excitatory input might advance the next burst of action potentials by hastening the positive feedback of voltage-dependent activation of calcium or sodium channels. Yet the same pulse of input might delay the next burst if it were to occur earlier, so as to slow the deactivation of those channels, or to slow the deactivation of potassium channels. So, one might expect that shortly before a spike or burst, excitatory input advances the oscillation, whereas shortly after a spike or burst, the same excitatory input delays the oscillation. Such behavior is shown in Figure 5.10 and can be seen in simulated neurons in Figure 5.11.

The phase response curve can be used to find whether an oscillator will entrain to a periodic input, and to determine the phase relationship of any eventual entrainment. If the oscillator has a longer period than the input, then, in order to entrain, it must receive sufficient phase advance in each cycle to reduce its period to that of the input. Conversely, if the oscillator's period is shorter than the input's then it must receive sufficient phase delay on each cycle in order to entrain.

Given the cyclic nature of phase response curves, any required level of advancement or delay can be reached at an even number (typically two) values of phase offset—for each offset at which the curve crosses a particular phase shift from below, there is another phase offset at which the curve re-crosses that particular phase shift from above. It turns out that only sections of the curve with negative gradient—so that the oscillator's phase advancement decreases, or its phase delay increases, with increasing phase delay of the input—can give rise to stable phase offsets (shaded regions of Figure 5.11).

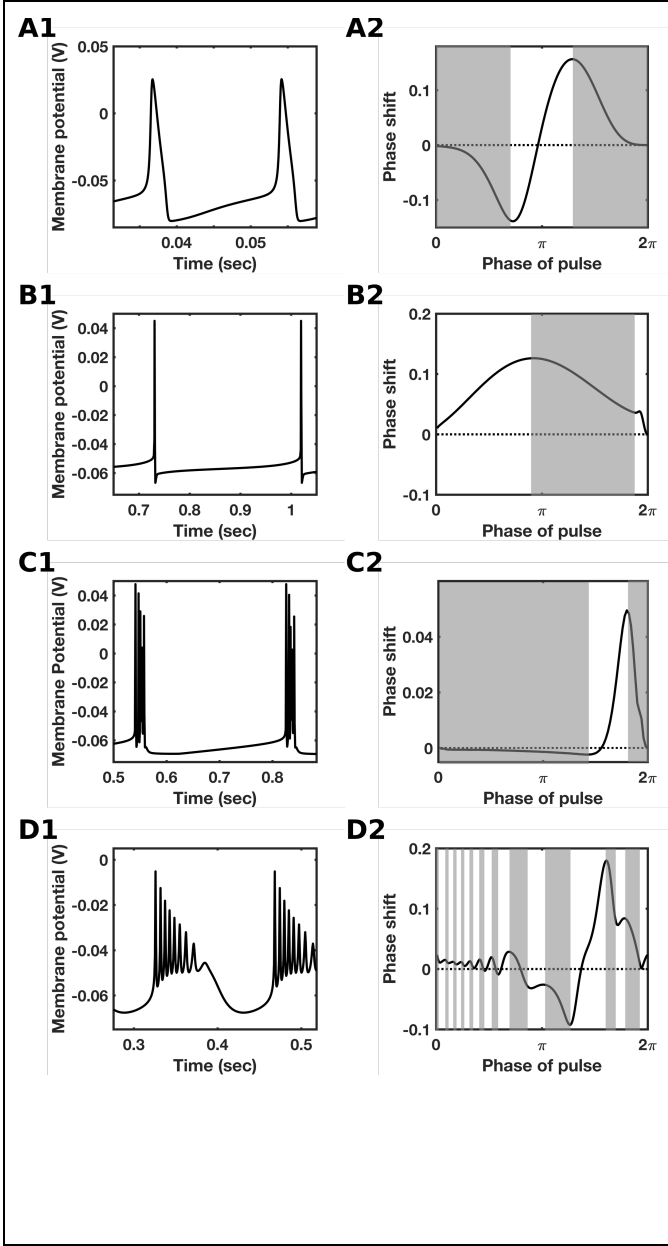


Figure 5.11. Phase response curves of simulated neurons. Model neurons in a regularly oscillating state (left) receive a 10pA pulse of excitatory current for 5ms at different points in their oscillating cycle, with a phase of 0 at the upswing of a spike or the first spike of a burst. Shaded regions on the right indicate where stable entrainment to a periodic sequence of such pulses is possible. **A.** Hodgkin-Huxley model, a Type-II neuron with biphasic PRC. **B.** Connor-Stevens model, a Type-I neuron with only phase-advance. **C.** The Pinsky-Rinzel model with current applied to the dendrite. While bi-phasic, the delay portion of the PRC is of longer duration and 20-fold smaller amplitude than the advance portion. **D.** The thalamic rebound model with altered parameters to render it regularly oscillating produces a more intricate PRC, with the timing of the pulse with respect to individual spikes within a burst impacting the phase shift, on top of a general delay then advance when input arrives between bursts. These panels are produced by the online codes **A:** Phase_Response_HH.m, **B:** Phase_Response_CS.m, **C:** Phase_Response_IHPR.m, **D:** Phase_Response_PIR.m.

To understand the stability requirement, consider a periodic input at a faster rate than an oscillator's natural frequency. Suppose the input on one cycle arrives at a phase offset that corresponds to a point on the curve with positive gradient and insufficient phase advancement to match the periodic input. Because the advancement of the oscillator is insufficient—*i. e.*, the oscillator has not been sped up enough to match the input—the next input will arrive earlier in the oscillator's cycle. The earlier input produces even less phase advancement for a later cycle, so the system moves away from the point of potential entrainment.

On the other hand, if insufficient phase advancement occurs at a phase offset where the phase response curve has negative gradient, then on the following cycle, the earlier arrival of the pulse produces greater phase advancement, so the oscillator approaches the

frequency of the inputs until it is entrained. If the oscillator receives too much advancement on one cycle, the input arrives at a slightly later phase on the following cycle, producing less advancement and slowing the oscillator relative to the inputs until it is entrained again.

When two or more oscillators are coupled, a similar analysis can be carried out to find the final phase relationship and eventual frequency of the coupled oscillators. The impact of each oscillator on each other must be considered. For two identical oscillators (A and B), the sum of phase offsets (A to B plus B to A) is, by necessity, 2π , or a multiple thereof.

When the two oscillators have identical phase response curves, the phase response of an offset angle, $\theta_{AB} = \theta$, must be identical to that at an offset angle of $\theta_{BA} = 2\pi - \theta$, in order for the two oscillators advance or delay by the same amount per cycle and remain entrained.

The requirement for stability in the previous section still holds, so the curve should have negative gradient for such a phase offset to be stable. Except in rare cases, the only possible stable solutions are $\theta_{AB} = \theta_{BA} = 0$ (in-phase or synchronous) or $\theta_{AB} = \theta_{BA} = \pi$ (out-of-phase or anti-phase). In the example of Figure 5.10, the phase-offset of 0 corresponds to a point of negative slope on the phase response curve, so is a stable phase-offset for excitatory coupling between these oscillators, whereas the phase-offset of π is unstable. However, if the coupling were inhibitory, the phase response curves would flip sign and the “in-phase” offset of 0 would be unstable, while the “anti-phase” offset of π would become the stable one. This is one account of the anti-phase behavior of many inhibition-coupled oscillators.

The resulting frequency of the coupled oscillators is obtained from the phase response curve by reading out the phase response, $\Delta\theta$, at the stable phase-offset. The phase response is calculated using the same units as the phase offset, so an advancement of 10% of a cycle corresponds to a phase response of $\Delta\theta = 0.1 \times 2\pi$. Since such an advance would occur on each cycle, the coupled frequency, f_c , would be 10% higher than the uncoupled frequency, f_u . In general, then, the coupled frequency is given by:

$$f_c = f_u \left(1 + \frac{\Delta\theta}{2\pi} \right). \quad \text{Eq. 5.11}$$

5.9. Tutorial 5.3: Bistability and oscillations from two LIF neurons.

Neuroscience goals: Learn how cross-inhibition can produce either oscillations or bistability in a single circuit, depending on synaptic properties (i. e., circuit structure does not determine behavior or function); observe how noise can produce transitions between activity states.

Computational goals: Keep track of two modeled neurons and be careful to use the output of one as the input of the other; record and plot the distribution of durations of states.

In this tutorial, you will couple together two leaky integrate-and-fire neurons with inhibitory synapses. We will see that if the inhibition is strong enough only one neuron can fire—as it fires it suppresses any activity in the other neuron. If we add noise, random switches in the active neuron arise. We will then see that adding short-term synaptic depression generates oscillations whose regularity is affected by the strength of noise. Similar models have been used to describe the alternations between percepts of visual or

auditory stimuli that are ambiguous, a phenomenon known as “perceptual rivalry” or “perceptual alternation” (Figure 5.8).

Set up the simulation to solve the following leaky integrate and fire equations for the membrane potentials, V_1 and V_2 , of the two cells, with synaptic gating variables, s_1 and s_2 , and depression variables, D_1 and D_2 , respectively:

$$C \frac{dV_1}{dt} = \frac{E - V_1}{R} + G_{21}s_2(E_{21}^{rev} - V_1) + I_1^{App} + \sigma \cdot \eta(t), \quad \frac{ds_1}{dt} = \frac{-s_1}{\tau_{syn}}, \quad \frac{dD_1}{dt} = \frac{1 - D_1}{\tau_D},$$

$$C \frac{dV_2}{dt} = \frac{E - V_2}{R} + G_{12}s_1(E_{12}^{rev} - V_2) + I_2^{App} + \sigma \cdot \eta(t), \quad \frac{ds_2}{dt} = \frac{-s_2}{\tau_{syn}}, \quad \frac{dD_2}{dt} = \frac{1 - D_2}{\tau_D}.$$

In the above equations, G_{12} and E_{12}^{rev} denote the maximal conductance and the reversal potential respectively, of the synapse from cell 1 to cell 2, while G_{21} and E_{21}^{rev} denote those properties of the other synapse (from cell 2 to cell 1). $\eta(t)$ is a white noise term of unit standard deviation (obtained by using the function “randn” in Matlab) and σ is the amplitude of noise (see Section 1.6.6 for noise implementation in the simulation). I_1^{App} and I_2^{App} are the applied currents to each cell, that will include a constant baseline term and a transient term to cause a switch.

Spikes are simulated as follows:

If $V_1 > V_{Th}$ then: $V_1 = V_R$, $s_1 \mapsto s_1 + p_R D_1 (1 - s_1)$ and $D_1 \mapsto D_1 (1 - p_R)$.

Similarly, if $V_2 > V_{Th}$ then: $V_2 = V_R$, $s_2 \mapsto s_2 + p_R D_2 (1 - s_2)$ and $D_2 \mapsto D_2 (1 - p_R)$.

PART A: BISTABILITY WITH NO SYNAPTIC DEPRESSION

- (i) Set the membrane capacitance, $C = 1nF$, the membrane resistance, $R = 10M\Omega$, the leak/reversal potential, $E = -70mV$, the threshold, $V_{Th} = -54mV$ and the reset potential $V_R = -80mV$ for each of the identical cells. Make the synapses identical and inhibitory, such that $E_{12}^{rev} = E_{21}^{rev} = -70mV$, $G_{12} = G_{21} = 1\mu S$, and $\tau_{syn} = 10ms$. Set the baseline applied current to be $2nA$. Set $p_R = 1$ and remove the effects of synaptic depression by ensuring that $D_1 = D_2 = 1$ throughout this simulation.
- (ii) Simulate the two, coupled neurons for a total time of 6s with an extra $3nA$ of applied current to one cell for the first 100ms of the simulation, then a pulse of $3nA$ to the other cell for 100ms at the midpoint of the simulation. Initially begin with no noise ($\sigma = 0$). Plot the membrane potential against time and the synaptic gating variables against time. Comment on your results.
- (iii) Now add noise by setting $\sigma = 50pA \cdot s^{-1/2}$ ($5 \times 10^{-11}A \cdot s^{-1/2}$)—that is, in each time step add a different random number to the current into the cell, using numpy’s `random.randn` function multiplied by $5 \times 10^{-11}/\sqrt{dt}$. Rerun the simulation with only the baseline current (no additional transient currents). Plot and comment on your results.
- (iv) Run the simulation for long enough to see over 1000 switches if you can and plot a histogram of the duration in each state—you will need to set a variable that records the state you are in and changes when the other cell spikes, at which point you record the time of state-switching. Taking differences in the switching times (use numpy’s “`diff`”) will produce a vector whose odd entries correspond to durations of one state and whose even entries correspond to durations of the other.

PART B: OSCILLATIONS WITH SYNAPTIC DEPRESSION.

- (v) Repeat (i) and (ii) but include the full effects of synaptic depression by setting $p_R = 0.2$ and updating the depression variables according to the equations above, with the time constant for recovery set as $\tau_D = 0.2\text{s}$. Plot and comment on your results.
- (vi) Add a small amount of noise, setting $\sigma = 5\text{pA.s}^{-1/2}$. Repeat (iv) and comment on any differences in the distribution of state durations between parts (iv) and (vi).

Questions for Chapter 5.

- 1) If the number of calcium channels at the axon terminals of a neuron were increased substantially, would the synapses near those terminals become more depressing, more facilitating, or neither? Explain.
- 2) What happens to the total conductance of a neuron's membrane and its effective time constant for change in the membrane potential when:
 - a) It receives a lot of excitatory synaptic input?
 - b) It receives a lot of inhibitory synaptic input?
- 3) A paired-pulse ratio is a measure of the synaptic transmission produced by a second action potential relative to that produced by an immediately preceding first action potential. If a synapse has 12 release-ready vesicles, a baseline release probability of $1/3$ and a facilitation factor of $1/3$, what is its paired-pulse ratio? Does this correspond to synaptic facilitation or depression?
- 4) In a simplified model of the CA3 region of the hippocampus of a rat, 250 000 excitatory pyramidal neurons connect with each other randomly with each possible connection present at a 1% probability. If one neuron excites any other neuron which also returns the excitation, we consider that neuron to be in a 2-step feedback loop.
 - a) What is the mean number of 2-step feedback loops per neuron?
 - b) What is the probability that a neuron has no such 2-step feedback loops and how many such neurons do you expect altogether in such a model of CA3?

5.10. Appendix: Synaptic input produced by a Poisson process

In this section, we will obtain mathematical expressions for how the synaptic input to neurons depends on presynaptic firing rate when biophysical processes such as saturation of receptors, synaptic depression, and synaptic facilitation are taken into account. Each process responds to a series of presynaptic events that are either the spikes or the release of vesicles. The mean effect of each of these processes alone can be calculated in response to either a regular series of events or, if the events are uncorrelated, as a Poisson process. Here we will derive the formulae for the response to a Poisson process. The results can be used in firing rate models (Chapter 6), which require the mean synaptic inputs as a function of presynaptic firing rates.

5.10.1. Synaptic saturation

To account for synaptic saturation, the synaptic response to each action potential is given by $s \mapsto s + \alpha p_r(1 - s)$, or equivalently by $s_+ = s_- + \alpha p_r(1 - s_-)$, where α is the fraction of unbound receptors bound following maximal vesicle release and p_r is the release probability for each vesicle following a spike. s is the fraction of synapses bound by neurotransmitter, which unbinds with a time constant, τ_s , such that $\tau_s \frac{ds}{dt} = -s$ between the times of spikes. s_+ denotes the value of s immediately after a spike and s_- denotes its value immediately before the spike. In this formulation α , which depends on the amount of neurotransmitter released per spike, is assumed to be constant and independent of spike history (*i.e.*, depression and facilitation are not included here).

When presynaptic spikes arrive so as to release vesicles as a Poisson process, the value of s is always fluctuating and the values of s_+ and s_- are different for every release event. However, by using the fact that the changes in s are linear functions of s , we can write equations for the mean values when the distribution of s has reached a steady state. In this case, using $\langle s \rangle$ to denote the mean of s , we can relate the mean value before and after a spike via:

$$\langle s_+ \rangle = \langle s_- \rangle + \alpha p_r(1 - \langle s_- \rangle). \quad \text{Eq. 5.12}$$

We also know that the dynamics of s between spikes is exponential decay such that

$$s_-^{(i+1)} = s_+^{(i)} \exp\left(-\frac{T_i}{\tau_s}\right) \quad \text{Eq. 5.13}$$

where $s_+^{(i)}$ is the value of s immediately after the i -th spike and T_i is the i -th inter-spike interval. We can now calculate the mean reduction in s between spikes by using the important Poisson property that the inter-spike interval, T_i , is independent of the prior value, $s_+^{(i)}$. Such independence means the average of the product of terms is equal to the product of their individual averages:

$$\begin{aligned} \langle s_- \rangle &= \langle s_-^{(i+1)} \rangle_i = \langle s_+^{(i)} \exp\left(-\frac{T_i}{\tau_s}\right) \rangle_i = \langle s_+^{(i)} \rangle_i \langle \exp\left(-\frac{T_i}{\tau_s}\right) \rangle_i \\ &= \langle s_+ \rangle \langle \exp\left(-\frac{T_i}{\tau_s}\right) \rangle_i. \end{aligned} \quad \text{Eq. 5.14}$$

The tricky term in Eq. 5.14, $\langle \exp\left(-\frac{T_i}{\tau_s}\right) \rangle_i$, requires an average over the inter-spike intervals, T_i . We use the Poisson formula for the probability distribution of inter-spike intervals, $P(T_i) = r \exp(-rT_i)$, where r is the rate of the Poisson process to obtain:

$$\begin{aligned}
\langle \exp\left(-\frac{T_i}{\tau_s}\right) \rangle_i &= \int_0^\infty \exp\left(-\frac{T}{\tau_s}\right) P(T) dT \\
&= \int_0^\infty \exp\left(-\frac{T}{\tau_s}\right) r \exp(-rT) dT \\
&= r \int_{r\tau_s}^\infty \exp\left(-T \frac{1+r\tau_s}{\tau_s}\right) dT \\
&= \frac{r\tau_s}{1+r\tau_s}.
\end{aligned} \tag{Eq. 5.15}$$

We can then insert this result into Eq. 5.14 to find

$$\langle s_- \rangle = \langle s_+ \rangle \frac{r\tau_s}{1+r\tau_s} \tag{Eq. 5.16}$$

and use Eq. 5.16 to substitute for $\langle s_- \rangle$ in Eq. 5.12 to obtain

$$\langle s_+ \rangle = \langle s_+ \rangle \frac{r\tau_s}{1+r\tau_s} + \alpha p_r \left(1 - \langle s_+ \rangle \frac{r\tau_s}{1+r\tau_s}\right). \tag{Eq. 5.17}$$

Some rearrangement leads to

$$\langle s_+ \rangle = \frac{\alpha p_r (1+r\tau_s)}{1+\alpha p_r r\tau_s} \tag{Eq. 5.18}$$

such that

$$\langle s_- \rangle = \frac{\alpha p_r r\tau_s}{1+\alpha p_r r\tau_s}. \tag{Eq. 5.19}$$

Interestingly, the overall mean value of s , $\langle s \rangle$, to be calculated below, is also $\frac{\alpha p_r r\tau_s}{1+\alpha p_r r\tau_s}$, the mean of the values of s immediately before an event, $\langle s_- \rangle$. This may seem counterintuitive because s is always higher as it decays to its value s_- just before the next event. However, the occurrences of a lower than average value of s_- follow longer intervals that contribute more to the mean value of s than do typical intervals. Since, for a Poisson process, an event can occur equally likely at any point in time, the value of a function immediately before an event is sampled equally across time, so the mean of values just before the event is equal to the mean across time.

For the aficionados, this result can be verified by a calculation that uses the average over an inter-spike interval, T , of an exponential decay:

$$\begin{aligned}
\langle \exp\left(-\frac{t}{\tau_s}\right) \rangle_T &= \frac{1}{T} \int_0^T \exp\left(-\frac{t}{\tau_s}\right) dt \\
&= \frac{\tau_s}{T} \left[1 - \exp\left(-\frac{T}{\tau_s}\right)\right]
\end{aligned} \tag{Eq. 5.20}$$

to obtain the weighted mean of this over all possible inter-spike intervals:

$$\int_0^\infty \langle \exp\left(-\frac{t}{\tau_s}\right) \rangle_T T P(T) dT \tag{Eq. 5.21}$$

$$\begin{aligned}
&= \langle s_+ \rangle r^2 \tau_s \left[\frac{1}{r} - \frac{\tau_s}{1 + r\tau_s} \right] \\
&= \langle s_+ \rangle \frac{r\tau_s}{1 + r\tau_s} \\
&= \frac{\alpha p_r r\tau_s}{1 + \alpha p_r r\tau_s} \\
&= \langle s_- \rangle.
\end{aligned}$$

In summary, the mean synaptic activation increases linearly with the presynaptic firing rate, r , when the firing rate is low ($r \ll 1/\alpha p_r \tau_s$), but synaptic activation saturates, approaching its maximum value of 1 at high firing rates ($r \gg 1/\alpha p_r \tau_s$).

5.10.2. Synaptic depression

Synaptic depression reduces the effective strength of a synapse temporarily when firing rates are high, because as we saw in the last section, the supply of release-ready vesicles gets depleted. We can quantify the mean effect of such depletion if presynaptic spikes arrive as a Poisson process of rate r and if the release probability, p_r , is held constant. The calculation is similar to the one for synaptic saturation (Section 5.10.1).

We can replace the factor, αp_r , the fraction of receptors bound following a presynaptic spike, by the factor $\alpha_0 D p_r$, where $0 < D \leq 1$ is the depression variable—*i.e.*, $\alpha = \alpha_0 D$. As we saw (Eq. 5.9a), the dynamics of D between spikes follows $\tau_D \frac{dD}{dt} = 1 - D$ and following each spike (Eq. 5.10), $D_+ = D_- (1 - p_r)$, where D_+ is the value of D immediately after and D_- the value of D immediately before the spike.

As in Section 5.10.1, we can consider the mean of values before and after spikes, writing

$$\langle D_+ \rangle = \langle D_- \rangle (1 - p_r) \quad \text{Eq. 5.22}$$

and using the solution for the value of D at a time t since the previous spike as

$$D(t) = 1 - (1 - D_-) \exp(-t/\tau_D) \quad \text{Eq. 5.23}$$

to produce

$$\langle D_- \rangle = 1 - (1 - \langle D_+ \rangle) \langle \exp(-T_i/\tau_D) \rangle, \quad \text{Eq. 5.24}$$

where the final term is averaged over all inter-spike intervals, T_i .

We use the result of Eq. 5.15 for a Poisson process of rate r ,

$$\langle \exp(-T/\tau_D) \rangle = \frac{r\tau_D}{1 + r\tau_D} \quad \text{Eq. 5.25}$$

to rewrite Eq. 5.24 as

$$\langle D_- \rangle = \frac{1}{1 + r\tau_D} + \langle D_+ \rangle \frac{r\tau_D}{1 + r\tau_D}. \quad \text{Eq. 5.26}$$

Using Eq. 5.22 to substitute for $\langle D_+ \rangle$ in Eq. 5.26 and rearranging leads to

$$\langle D_- \rangle = \frac{1}{1 + p_r r\tau_D}. \quad \text{Eq. 5.27}$$

It is this value, representing the fraction of the complete stock of release-ready vesicles present when an action potential arrives, that determines the amount of neurotransmitter released and the synaptic efficacy. At low rates, $r \ll 1/p_r \tau_D$, $\langle D_- \rangle$ is approximately equal to one, but at high rates, $r \gg 1/p_r \tau_D$, $\langle D_- \rangle$ decays inversely with rate. Therefore, at high rates the total synaptic transmission of $\alpha_0 p_r \langle D_- \rangle r\tau_s = \frac{\alpha_0 p_r r\tau_s}{1 + p_r r\tau_D}$ (ignoring synaptic saturation) approaches, but never exceeds a maximum value of $\alpha_0 \tau_s / \tau_D$.

5.10.3. Synaptic facilitation

The term for synaptic facilitation, F , scales the vesicle-release probability, $p_r = Fp_0$, where p_0 is the baseline value, so it also provides a multiplicative contribution to the fraction of receptors bound per spike. The dynamics of F between spikes is identical to the dynamics of D —namely an exponential decay toward 1—but with a time constant of τ_F and with the understanding that $F(t) \geq 1$ for all t . Therefore, the calculation for the average over an exponential decay to 1, relating the mean value of F immediately before a spike to its mean value immediately following a spike leads to a similar result to the one for depression (Eq. 5.26):

$$\langle F_- \rangle = \frac{1}{1 + r\tau_F} + \langle F_+ \rangle \frac{r\tau_F}{1 + r\tau_F}. \quad \text{Eq. 5.28}$$

The change in F following a spike (Eq. 5.10), $F_+ = F_- + f_{fac}(F_{max} - F)$ allows us to write

$$\langle F_+ \rangle = \langle F_- \rangle (1 - f_{fac}) + f_{fac}F_{max}. \quad \text{Eq. 5.29}$$

Using Eq. 5.29 to substitute for $\langle F_+ \rangle$ in Eq. 5.28 and rearranging leads to

$$\begin{aligned} \langle F_- \rangle &= \frac{1 + f_{fac}F_{max}r\tau_F}{1 + f_{fac}r\tau_F} \\ &= 1 + \frac{(F_{max} - 1)f_{fac}r\tau_F}{1 + f_{fac}r\tau_F}. \end{aligned} \quad \text{Eq. 5.30}$$

At low rates ($r \ll 1/f_{fac}\tau_F$) the facilitation factor, $\langle F_- \rangle$, increases from 1 linearly with firing rate and at high firing rates ($r \gg 1/f_{fac}\tau_F$) $\langle F_- \rangle$ approaches its maximum possible value, F_{max} .

5.10.4. Notes on combining mechanisms

The derivations for each of the three mechanisms above rely on the incoming series of events being Poisson processes. However, once mechanisms are combined the Poisson assumption can no longer hold. For example, if presynaptic spikes arrive as a Poisson process but there is synaptic facilitation then vesicles are not released as a Poisson process. In fact, facilitation tends to increase the coefficient of variation of release events, increasing the relative probability of very short intervals at the same time as increasing the relative probability of very long intervals between vesicle-release times compared to a Poisson time series. This is because release is more likely after a short interval than on average, enhancing the number of short intervals, while release is less likely after a long interval, which makes long intervals even longer. Conversely, synaptic depression tends to even out the intervals between times of vesicle release as fewer vesicles are available to be released shortly after a period of high release rate, but more can be released when release-rate is low.

Given the inappropriateness of the Poisson formulae for the complete synaptic dynamics, alternative approaches are either: 1) to improve the calculations by including the correlations induced at each stage; or 2) simply to simulate a single synapse and empirically fit the mean response (and perhaps also its fluctuations) as a function of presynaptic rate. Such fitting can be carried out for any fixed set of parameters (time constants, facilitation factor, base release probability) but has the disadvantage that for any

change in underlying parameters a new set of simulations are required to fit the output before the firing rate model can be updated.

References for Chapter 5

1. Stanley EF. The Nanophysiology of Fast Transmitter Release. *Trends Neurosci.* 2016;39(3):183-197.
2. Surmeier DJ, Ding J, Day M, Wang Z, Shen W. D1 and D2 dopamine-receptor modulation of striatal glutamatergic signaling in striatal medium spiny neurons. *Trends Neurosci.* 2007;30(5):228-235.
3. Seamans JK, Yang CR. The principal features and mechanisms of dopamine modulation in the prefrontal cortex. *Prog Neurobiol.* 2004;74(1):1-58.
4. Prinz AA, Bucher D, Marder E. Similar network activity from disparate circuit parameters. *Nat Neurosci.* 2004;7(12):1345-1352.
5. Sharp AA, O'Neil MB, Abbott LF, Marder E. Dynamic clamp: computer-generated conductances in real neurons. *J Neurophysiol.* 1993;69(3):992-995.
6. Abbott LF, Regehr WG. Synaptic computation. *Nature.* 2004;431(7010):796-803.
7. Tsodyks M, Wu S. Short-term synaptic plasticity. *Scholarpedia.* 2013;8(10):3153.
8. Hennig MH. Theoretical models of synaptic short term plasticity. *Front Comput Neurosci.* 2013;7:154.
9. Zucker RS, Regehr WG. Short-term synaptic plasticity. *Annual Review of Physiology.* 2002;64:355-405.
10. Abbott LF, Varela JA, Sen K, Nelson SB. Synaptic depression and cortical gain control. *Science.* 1997;275(5297):220-224.
11. Mongillo G, Barak O, Tsodyks M. Synaptic theory of working memory. *Science.* 2008;319(5869):1543-1546.
12. Dayan P, Abbott LF. *Theoretical Neuroscience.* MIT Press; 2001.
13. Ikeda K, Bekkers JM. Autapses. *Curr Biol.* 2006;16(9):R308.
14. Song S, Sjöström PJ, Reigl M, Nelson S, Chklovskii DB. Highly nonrandom features of synaptic connectivity in local cortical circuits. *PLoS Biol.* 2005;3(3):e68.
15. Perin R, Berger TK, Markram H. A synaptic organizing principle for cortical neuronal groups. *Proc Natl Acad Sci U S A.* 2011;108(13):5419-5424.
16. Rubin E. *Synsoplevede Figurer: Studier i psykologisk Analyse. Forste Del [Visually experienced figures: Studies in psychological analysis. Part one].* Copenhagen and Christiania: Gyldendalske Boghandel, Nordisk Forlag, University of Copenhagen; 1915.
17. Jastrow J. The mind's eye. *Popular Science Monthly.* 1899;54:299-312.
18. Wang XJ, Rinzel J. Alternating and synchronous rhythms in reciprocally inhibitory model neurons. *Neural Comput.* 1992;4:84-97.
19. Marder E, Bucher D, Schulz DJ, Taylor AL. Invertebrate central pattern generation moves along. *Curr Biol.* 2005;15(17):R685-699.
20. Calabrese RL, Nadim F, Olsen OH. Heartbeat control in the medicinal leech: a model system for understanding the origin, coordination, and modulation of rhythmic motor patterns. *J Neurobiol.* 1995;27(3):390-402.
21. Calabrese RL, De Schutter E. Motor-pattern-generating networks in invertebrates: modeling our way toward understanding. *Trends Neurosci.* 1992;15(11):439-445.
22. Marder E, Haddad SA, Goeritz ML, Rosenbaum P, Kispersky T. How can motor systems retain performance over a wide temperature range? Lessons from the crustacean stomatogastric nervous system. *J Comp Physiol A Neuroethol Sens Neural Behav Physiol.* 2015;201(9):851-856.

23. Buchanan JT. Lamprey spinal interneurons and their roles in swimming activity. *Brain Behav Evol.* 1996;48(5):287-296.
24. Zhang C, Guy RD, Mulloney B, Zhang Q, Lewis TJ. Neural mechanism of optimal limb coordination in crustacean swimming. *Proc Natl Acad Sci U S A.* 2014;111(38):13840-13845.
25. Stiefel KM, Ermentrout GB. Neurons as oscillators. *J Neurophysiol.* 2016;116(6):2950-2960.